Progress in Retinal and Eye Research 59 (2017) 178–201

Contents lists available at ScienceDirect

Progress in Retinal and Eye Research

journal homepage: www.elsevier.com/locate/prer

The application of optical coherence tomography angiography in uveitis and inflammatory eye diseases

Francesco Pichi, MD [a, b, *], David Sarraf, MD [c, d], Sruthi Arepalli, MD [b], Careen Y. Lowder, MD, PhD [b], Emmett T. Cunningham Jr., MD, PhD, MPH [e, f, g, h], Piergiorgio Neri, MD, PhD [i], Thomas A. Albini, MD [j], Vishali Gupta, MD [k], Kimberly Baynes, RN [b], Sunil K. Srivastava, MD [b]

[a] Cleveland Clinic Abu Dhabi, Abu Dhabi, United Arab Emirates
[b] Cole Eye Institute, Cleveland Clinic, Cleveland, OH, USA
[c] Stein Eye Institute, University of California, Los Angeles, Los Angeles, CA, USA
[d] Greater Los Angeles VA Healthcare Center, Los Angeles, CA, USA
[e] The Department of Ophthalmology, California Pacific Medical Center, San Francisco, CA, USA
[f] The Department of Ophthalmology, Stanford University School of Medicine, Stanford, CA, USA
[g] The Francis I. Proctor Foundation, UCSF School of Medicine, San Francisco, CA, USA
[h] West Coast Retina Medical Group, San Francisco, CA, USA
[i] The Ocular Immunology Service, The Eye Clinic, Polytechnic University of Marche, Ancona, Italy
[j] Bascom Palmer Eye Institute, University of Miami-Miller School of Medicine, Miami, FL, USA
[k] Advanced Eye Centre, Post Graduate Institute of Medical Education and Research, Chandigarh, India

ARTICLE INFO

Article history:
Received 9 November 2016
Received in revised form
10 April 2017
Accepted 11 April 2017
Available online 29 April 2017

Keywords:
Optical coherence tomography angiography
Anterior uveitis
Chorioretinal inflammation

ABSTRACT

Since its introduction in the early 1990s, optical coherence tomography (OCT) has evolved in resolution and technological advances, and in recent years its initial application of assessing the morphology of a tissue has been implemented by the study of its functional blood flow, through optical coherence tomography angiography (OCTA). This novel technique details capillary networks by comparing the amount of light returned from static and moving targets without the need for intravenous dye administration. While this imaging modality has been used for various ocular conditions, the application OCTA to uveitis conditions remains sparse.

This review aims to establish the basis of OCTA and its current application to ocular inflammatory disorders, with an emphasis on monitoring progression and response to treatment, as well as predicting visual complications. In particular, this review explores the use of OCTA in iris vessel dilation seen in various forms of iritis, as a predictive factor for further episodes of inflammation. OCTA can also depict ischemia in the deep plexus layers of the retina and identify true choroicapillaris ischemia in cases of placoid diseases or masking of the indocyanine green dye, as in multiple evanescent white dot syndrome. In addition, OCTA can depict neovascularization in granulomatous disease of the retina or choroid not previously depicted with previous imaging methods. While OCTA provides several advancements in the imaging, management and prognosis of uveitis diseases, we emphasize that further studies are required to fully understand its application to these conditions.

© 2017 Elsevier Ltd. All rights reserved.

Contents

* Corresponding author. Cleveland Clinic Abu Dhabi, Al Falah Street, Al Maryah Island, Abu Dhabi, United Arab Emirates.
E-mail address: ilmiticopicchio@gmail.com (F. Pichi).

http://dx.doi.org/10.1016/j.preteyeres.2017.04.005
1350-9462/© 2017 Elsevier Ltd. All rights reserved.

1. Introduction

The intraocular vascular networks are complex, multilayered and critical to ocular function (Gorczynska et al., 2016). Intraocular inflammation can be associated with various vascular flow abnormalities in a wide spectrum of uveitic disorders. Recognizing patterns of disruption is integral to the diagnosis and management of these conditions. In uveitic conditions in particular, abnormal flow has been documented in the iris (Pichi et al, 2016a) in patients with acute anterior uveitis, in the inner retina (birdshot chorioretinopathy) (Phasukkijwatana et al., 2016), in the inner choroid (acute posterior multifocal placoid pigment epitheliopathy) (Klufas et al., 2017; Salvatore et al., 2016) and in the outer choroid (birdshot chorioretinopathy (Phasukkijwatana et al., 2016), multifocal choroiditis (Cerquaglia et al., 2016), vogt-koyanagi-harada disease (Aggarwal et al., 2016), and tuberculosis [Agarwal et al., 2016]). Various imaging modalities exist, including optical coherence tomography (OCT), optical coherence tomography angiography (OCTA), fluorescein angiography (FA) and indocyanine green angiography (ICGA). This review aims to discuss the imaging modalities previously used for uveitis and review the importance of OCTA as an advanced tool for the evaluation of uveitic conditions.

1.1. Dye-based angiography of the vasculature of the eye

The gold standard modalities for the imaging of retinal and choroidal vessel morphology are fluorescein angiography (FA) and indocyanine green angiography (ICGA) (Gorczynska et al., 2016), but these procedures are invasive and require the injection of an intravenous dyes that may be poorly tolerated and associated with rare serious side effects (Yannuzzi et al., 1986; Hope-Ross et al., 1994). These imaging techniques are, in addition, time and labor intensive and require the skilled administration of contrast agents and the capture of flow at appropriate time frames. Further, leakage with IVFA can obscure the identification of morphological vascular detail, and window defects can prevent accurate analysis of retinal detail. The ICG molecule on the other hand is normally absorbed by the healthy RPE, contributing to the physiological background hyperfluorescence (Chang et al., 2005). RPE mottling or disruption of the ellipsoid zone can produce areas of hypofluorescence that may be misinterpreted as being located in the choroid.

Moreover, these modalities provide two dimensional evaluation of the retina and choroid and are unable to identify the level of vascular abnormalities. These drawbacks limit the routine use of dye-based angiography during each clinical visit for patients to monitor for disease presence and progression.

1.2. Optical coherence tomography angiography

Optical coherence tomography angiography has emerged a non-invasive alternative technique for the imaging of the retinal and choroidal vasculature (Fingler et al., 2007). It provides an accurate depiction of the microvasculature morphology of the retinal and choroidal blood vessels, without obscuration from leakage. This allows monitoring of disease processes in situations where vascular details can be obscured by leakage. Moreover, OCTA allows for segmentation of retinal and choroidal layers and localization of abnormalities (Fingler et al., 2008). The basis of OCTA relies on the reflectance of a light source off the surface of moving blood cells, eliminating the need for dyes.

OCTA is an expansion off the imaging processes of SD-OCT, in order to visualize flow through different segmented areas of ocular tissue. (Spaide et al, 2015a). OCT, in brief, is an imaging modality which creates cross-sectional representations of tissue from various, consecutive scans at varying depths. Initially, OCT images were gathered through time-domain detection, but later

advancements in imaging have led to spectral domain, and swept source which are faster than the original methods (White et al., 2003). These methods rely on simultaneous analysis of tissue reflectance, rather than relying on sequential imaging, which is time-intensive (Bachmann et al., 2007).

OCTA relies on repeatedly imaging the same area of tissue multiple times, and analyzing differences between scans of the same area to assess flow. (Spaide et al, 2015a). This is based on the premise that areas that contain high rates of flow will have large changes between each scan, while areas with slower, or no flow, will remain closer to previous scans of the same area. (Spaide et al, 2015a). Two main types of wavelengths can be utilized to generate these representations of flow. Spectral domain OCT utilizes a shorter wavelength, near 800 nm, while swept source OCT uses wavelengths closer to 1050 nm (Leitgeb et al., 2004). Shorter wavelengths penetrate less and cause more scatter from media opacities, while longer wavelengths have a higher penetrance through deeper tissue, but a slightly lower axial resolution (Spaide et al, 2015a).

The light emitted from the OCT device can either be reflected, or lost, through refraction or absorption (Spaide et al, 2015a). OCTA uses this principle of OCT to detect motion contrast through the application of either of 2 main methods: speckle or amplitude decorrelation (also referred to as intensity) or phase variance. Amplitude decorrelation assesses the difference in amplitudes over time between 2 different OCT B scans over the same area to calculate motion (Spaide et al, 2015a). Phase variance is based on the light wave property of an emitted light source, and the phase variation caused when the light makes contact with moving objects. Variations over multiple scans with the received light source indicate motion when it is above a certain threshold which signifies background noise.

The above two methods depict motion by comparing the difference in light reflections hitting various vessels from the background in order to determine if there is significant motion. Small movements of the eye, either from saccades, variation in cardiac rhythm, or small changes in fixation can induce significant background noise and disrupt the ability of OCTA to depict true pathological flow. In order to improve visualization and minimize background noise from small movements, two averaging methods have been developed: the split spectrum amplitude decorrelation technique and volume averaging (Gorczynska et al., 2016; Jia et al., 2012). The split spectrum amplitude decorrelation technique divides an acquired image into an exponentially greater number of B scans thereby significantly amplifying the decorrelation analysis. While this averaged technique, reduces background noise and improves visualization of the retinal and choroidal vasculatures, axial resolution may be lost (Jia et al., 2012). Volume averaging relies on the acquisition of multiple OCTA data sets, and removing artifacts thought to be secondary to movement and re-averaging the corrected OCTA volumes (Gorczynska et al., 2016). Given the dependence of OCTA on the penetrance of a light source, artifacts arise from limitation of this function. Shorter wavelengths have decreased penetrance through deeper structures, while longer wavelengths lose axial resolution (Spaide et al, 2015a). Moreover, media opacities such as cataracts and pathological abnormalities such as choroidal neovascularization, or placoid chorioretinitis lesions or chorioretinal granuloma, as are found in AMPPE or tuberculosis, can cause signal attenuation and blockage of the underlying vasculature referred to as a shadowing artifact (Spaide et al, 2015a). In addition, light can strike the tissue beneath a blood vessel and become reflected back, mimicking the pattern of the overlying blood vessel, and creating a projection artifact. Small transverse movements, such as fixation changes or eye movements associated with the cardiac cycle or tremor or breathing can also induce artifacts, which are difficult to correct and referred to as false positive flow (Spaide et al, 2015a). These could be potentially decreased with eye tracking software to mitigate these effects. To reduce this artifact generation, OCTA algorithms incorporate a threshold for flow signal detection but this may limit the detection of slow flow areas, causing a false negative flow, below the established threshold level. Moreover, the limited view available with OCTA imaging (8 mm × 8 mm), prevents a wide fundus evaluation of various disease processes.

Among the commercially available OCTA devices, the most frequently used are mainly four.

ZEISS Angioplex™ OCT angiographic imaging on the CIRRUS™ HD-OCT platform was made possible by increasing the scanning rate to 68,000 A-scans per second and introducing improved tracking software known as FastTrac™ retinal-tracking technology. The generation of en face microvascular flow images with Angioplex™ OCT uses an algorithm known as OCT microangiography-complex, which incorporates differences in both the phase and intensity information contained within sequential B-scans performed at the same position. A volumetric dataset showing erythrocyte flow information can then be displayed as a color-coded retinal depth map in which the microvasculature of the superficial, deep, and avascular layers of the retina are displayed together.

Optovue AngioVue system technology is based on the AngioVue Imaging System (Optovue, Inc., Freemont, CA), using split-spectrum amplitude-decorrelation angiography (SSADA) algorithm. This algorithm was developed to minimize scanning time. The novelty of SSADA lies in how the OCT signal is processed to enhance flow detection and reject axial bulk motion noise. Specifically, the algorithm splits the OCT image into different spectral bands, thus increasing the number of usable image frames. Each new frame has a lower axial resolution that is less susceptible to axial eye motion caused by blood pulsation. Optovue AngioVue system technology allows quantitative analysis. It provides numerical data about flow area and non-flow area. It can also generate a flow density map based on an ETDRS grid centered on the macula.

Topcon has recently developed an innovative OCTA algorithm, OCTARA (OCTA Ratio Analysis), which benefits from being paired with swept-source OCT. OCTARA aims to provide improved detection sensitivity of low blood flow and reduced motion artifacts without compromising axial resolution.

Heidelberg engineering applies its active eye-tracking (TruTrack™) that uses the simultaneous acquisition of fundus and OCT images to reduce motion artifacts and improve signal-to-noise ratio.

2. Optical coherence tomography of the iris in anterior uveitis

The term “anterior uveitis” encompasses all types of uveitis in which the predominant site of inflammation involves the iris and the ciliary body (Jabs et al., 2005). Inflammatory cells are therefore seen in the anterior chamber (iritis) or in the anterior chamber and anterior vitreous in the retrolental space (iridocyclitis) (Dunn, 2015). While the ciliary body is not visible, the iris can be easily visualized (Peizeng et al., 2009). The dilation of iris vessels in anterior uveitis is well documented, and OCTA presents a possible objective measurement of ocular inflammation. Previous attempts to identify and measure iris vessel dilation in uveitis have been limited to anterior segment fluorescein angiography (Brancato et al., 1997; Danzig et al., 2008). However, fluorescein angiography studies of the iris in uveitis have been abandoned for the last decade (Brancato et al., 1997; Wiechens and Nölle, 1999).

2.1. Optical coherence tomography angiography of the iris in murine models

Choi et al. (2015) were the first to apply OCT-based microangiography to an acute anterior uveitis model in rats. They initiated anterior uveitis in 2 female Lewis with an intravitreal injection of 10 μg of killed mycobacterium tuberculosis antigen. To assess the effect of treatment of uveitis on iris vasculature, one of the rat was treated with a periocular injection of 4 mg triamcinolone in 0.1 ml. They then imaged blood flow in the irises of these rodents through an OCTA algorithm. Their OCTA results showed that the iris vessels became dilated 2 days after induction of anterior uveitis while the limbal circulation was not affected. To quantify their amount of vascular dilation Choi et al. (2015) compared manually measured iris vessel diameters at the same location for the pre and post-injection OCT angiograms. On average, the vessel diameters at day 2 were 30–40% greater than those at day 0.

2.2. Optical coherence tomography angiography of the iris in human anterior uveitis

From a rodent model with manual measurements, Pichi et al. (2016a) were the first to objectively quantify iris vasculature through OCTA in thirty-five patients with acute anterior uveitis. Pre-dilation OCTA scans of the irises were performed with Optovue RTVue XR Avanti (Optuvue, Inc, Fremont, CA) and focus settings were increased to +28 D in order to position the iris tissue within the depth of focus of the beam. The iris microvasculature was better highlighted in acute anterior uveitis eyes compared to non-inflamed irises, with densely packed radial small vessels towards the center of pupil and irregular less densely packed vessels towards the iris root.

2.2.1. Basic optical coherence tomography angiography anatomy of iris vasculature

A single branch of a long posterior ciliary artery (LPCA in Fig. 1) traveling almost perpendicular to the radial vessels could be seen in 77% of the uveitic irises, near the iris root. Major arterial circles were observed extending from the iris root toward the pupillary margin (Fig. 1, arrows), where they branch into the lesser iris circles (Fig. 1, arrow heads). At the root of the iris an hyperreflective band (Fig. 1, asterisks) run almost continuously, representing the limbal circulation. Anterior to that the ciliary circulation is obscured due to the fact that the vessels dive deep towards the ciliary bodies thus being below the focal plane in our imaging study.

2.2.2. Quantitative analysis based on iris vessels brightness

To quantify the amount of flow increase and vessels dilation that occurs with anterior inflammation, Pichi et al. (2016a) compared brightness of the grayscale renderings of pre and post-treatment OCT angiograms. Post-image acquisition analysis on all OCTA of the iris was performed through ImageJ, (https://imagej.nih.gov/ij/). The measurement procedure included obtaining the ROI within the pupil and the iris root. All images were converted to an 8-Bit grayscale calculated by converting each RGB image into a grey scale value using the following formula: $V = 0.299R + 0.587G + 0.114B$ (V = Y; R = red; G = green; B = blue) (Hartig, 2013; Kang and Kim, 2014). Brightness was then adjusted in a standardized way in order to highlight only the bright vessels. Reflectivity (highlighted in white) was measured with the ImageJ software, which converts grey scale images to intensity per pixel to calculate reflectivity values (Fig. 2). Mean brightness in eyes with 4 + cells was 61.5 ± 13.4, in eyes with 3 + cells it was 44.1 ± 9.7, in eyes with 2 + cells it was 21.8 ± 16.3 and finally in 1 + cells eyes the mean brightness in pixels was 17.9 ± 7.2.

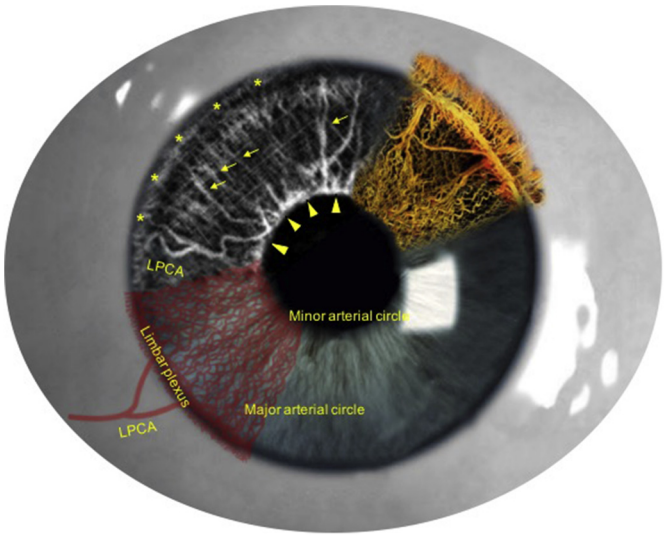

Fig. 1. *Optical coherence tomography angiography anatomy of inflamed iris vessels.* This schematic representation of the human iris has an OCTA scan of its vessels superimposed on top left, and an electron microscopy on the top right (Kim et al., 2016). On the OCTA scan, a single branch of a long posterior ciliary artery (LPCA) in the vicinity of the iris root gives rise to a major arterial circle (arrows) traveling almost perpendicular in the iris body. In the pupillary margin, the lesser iris circles (arrow heads) are clearly visible, bridging adjacent vascular networks. At the root of the iris an hyperreflective band (asterisks) runs almost continuously, representing the limbal circulation. Anterior to that the ciliary circulation is obscured due to the fact that the vessels dive deep towards the ciliary bodies thus being below the focal plane of the optical coherence tomography. The figure highlights the correspondence between iris vessels anatomy on electron microscopy and on OCTA, and gives a schematic rendering of the vasculature on bottom left.

2.2.3. Quantitative analysis based on automated algorithm

OCTA images of the iris (Fig. 3, panel A) are processed using a combination of 3D Gaussian filters, spectral bandpass filters, intensity thresholding and 3D morphological "opening" filters (Fig. 3, panel B) to remove non-specific, non-contiguous voxels and segment bright, connected voxels representing vessel segments (Fig. 3, panel C). Vascular volumes are subsequently calculated by summing voxels in the resulting vessel masks. A mean 3 × 3 vascular iris volume in patients with 4 + anterior chamber cells was 0.28 mm^3, in 3 + cells 0.19, in 2 + cells 0.11, in 1 + cells 0.08 (Fig. 4).

These preliminary data show the utility of OCTA in analyzing the iris vasculature from a qualitative and quantitative point of view. A proper development of OCTA for the anterior segment may open the doors to its use in other systemic and ocular conditions, such as vasculitis and diabetes. However, at present there are several limitations to the employment of OCTA to analyze iris vessels in a reproducible way. First of all, the iris vasculature caliber and tortuosity could be affected by pupillary dilation. Although the studies reported employed the same lighting conditions (ambient illumination) for all exams, a variation in pupil size is inevitable due to accommodation. The pupil size needs to be constant through all imaging sessions to minimize the effect due to environmental factors that may affect iris vasculature calibers, so that the quantitative measurements of iris vessel diameter in inflammation and treatment can be reproducible. Secondly, differences in irises pigmentation among patients may bias the OCTA measurement. Finally, for anterior OCT imaging ocular tissue refraction of the OCT beam can distort the physical geometry of the anterior segment in an OCT image. The reliability of the quantitative parameters reported can be improved with correction of the optical distortion considering the refractive indices of ocular tissue layers. Further studies may be needed to confirm that refraction does not change

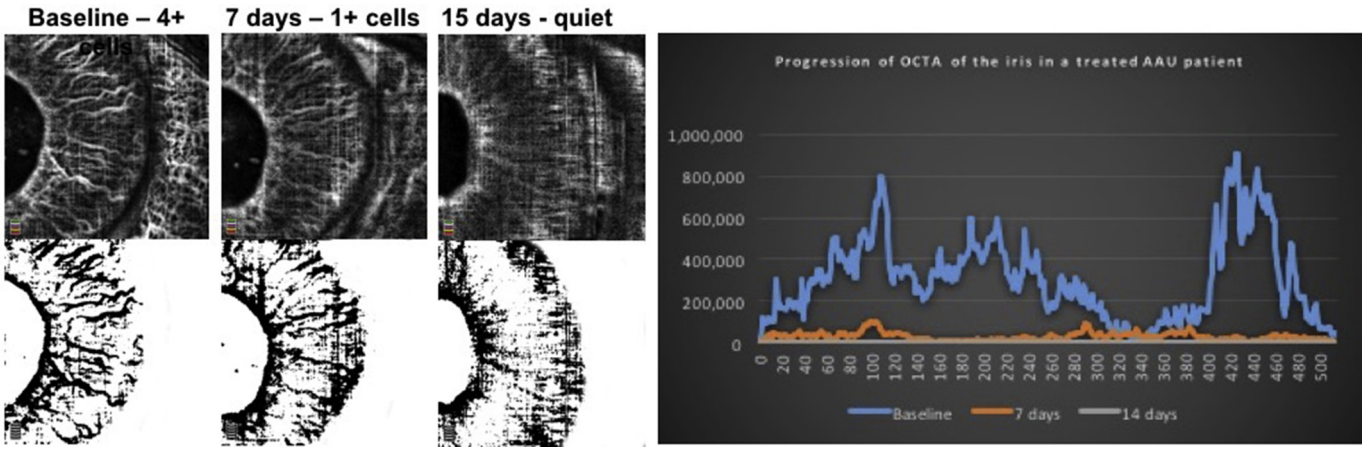

Fig. 2. *Optical coherence tomography angiography of the iris in an active anterior uveitis patient highlights the progressive decrease of the vessels caliper and dilation with control of inflammation.* A 36-years-old patient with acute anterior uveitis examined with OCTA of the iris at baseline (4 + cells), after 7 days of prednisolone acetate 1% every 2 h (2 + cells) and at 15 days (quiet). The progressive decrease in the caliper of the vessels is qualitatively visible in the greyscale rendering (bottom row) and is confirmed by the histogram (right panel) that compares point-by-point pixels reflectance of the iris vessels when inflamed (blue line), when less inflamed (orange) and quiet (flat grey line). This anterior uveitis patient is the perfect example of how OCTA of the iris can detect inflammation through dilation of the iris vessels.

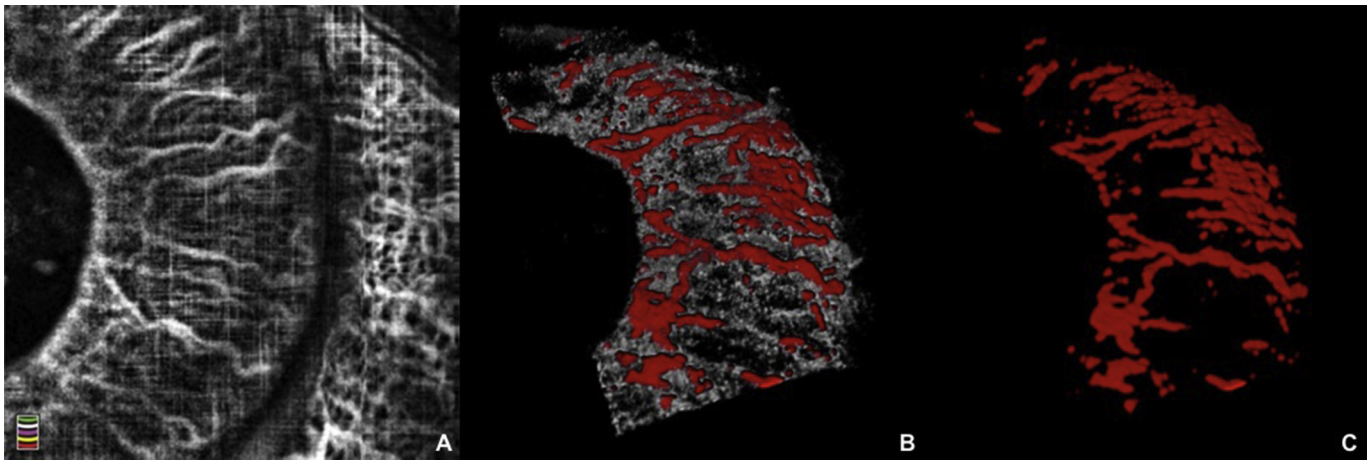

Fig. 3. *Automated algorithm to measure iris vessels volume using OCTA in patients with acute anterior uveitis.* A 3 × 3 OCT angiogram of the nasal iris of a patient with 3 + anterior chamber cells is shown in panel A. A 3D cube is processed using a combination of 3D Gaussian filters, spectral bandpass filters, intensity thresholding and 3D morphological "opening" filters to remove non-specific, non-contiguous voxels (B). Connected voxels represent vessel segments. Vascular volumes were subsequently calculated by summing voxels in the resulting vessel masks (C).

with improvement in the degree of ocular inflammation or with treatment with steroids.

3. Optical coherence tomography angiography of infectious and inflammatory granulomas

The term "granuloma" refers to a nodular collection of immune cells, usually macrophages and epithelioid cells encircled by lymphocytes. They are formed by the immune system to confine pathogens and inflammatory agents that cannot be eliminated. Clinically, inflammatory masses in the anterior and/or posterior chamber are often referred to as "granulomas" even in the absence of histological demonstration of the defining presence of epithelioid or giant cell formation.

3.1. Granulomas of the retina

Retinal granulomas can be associated with infectious and inflammatory ocular and systemic diseases. Among the inflammatory eye conditions that can manifest with retinal granulomas, sarcoidosis is by far the most common (Spagnolo, 2015). Sarcoidosis is an idiopathic multisystem granulomatous inflammatory disorder, and ocular involvement is seen in about 30–50% of patients. Biopsy of pulmonary or lacrimal gland sarcoid granulomas shows discrete non-caseating granulomas occasionally with central necrosis. The giant cells within the reaction are of foreign body type. These giant cells and the epithelioid cells may contain or surround *Schaumann bodies* – basophilic spherical or ovoid bodies of calcium oxalate, or *asteroids* – small acidophilic star-shaped bodies, also of calcium oxalate. Retinal sarcoid granulomata appear as grey-white nodules. "Lander's sign" is denoted to describe extension of sarcoid granulomata onto the retinal surface and into the vitreous.

A granulomatous reaction will surround foci of Toxoplasma gondii retinitis (Maenz et al., 2014). It is a focal granulomatous necrotizing retinitis. The granulomas may have a necrotic center which is surrounded by epithelioid cells and a variable infiltrate of giant cells, lymphocytes and plasma cells. The retinal cysts and free parasites (in active disease) can be seen within the retinal cells. The

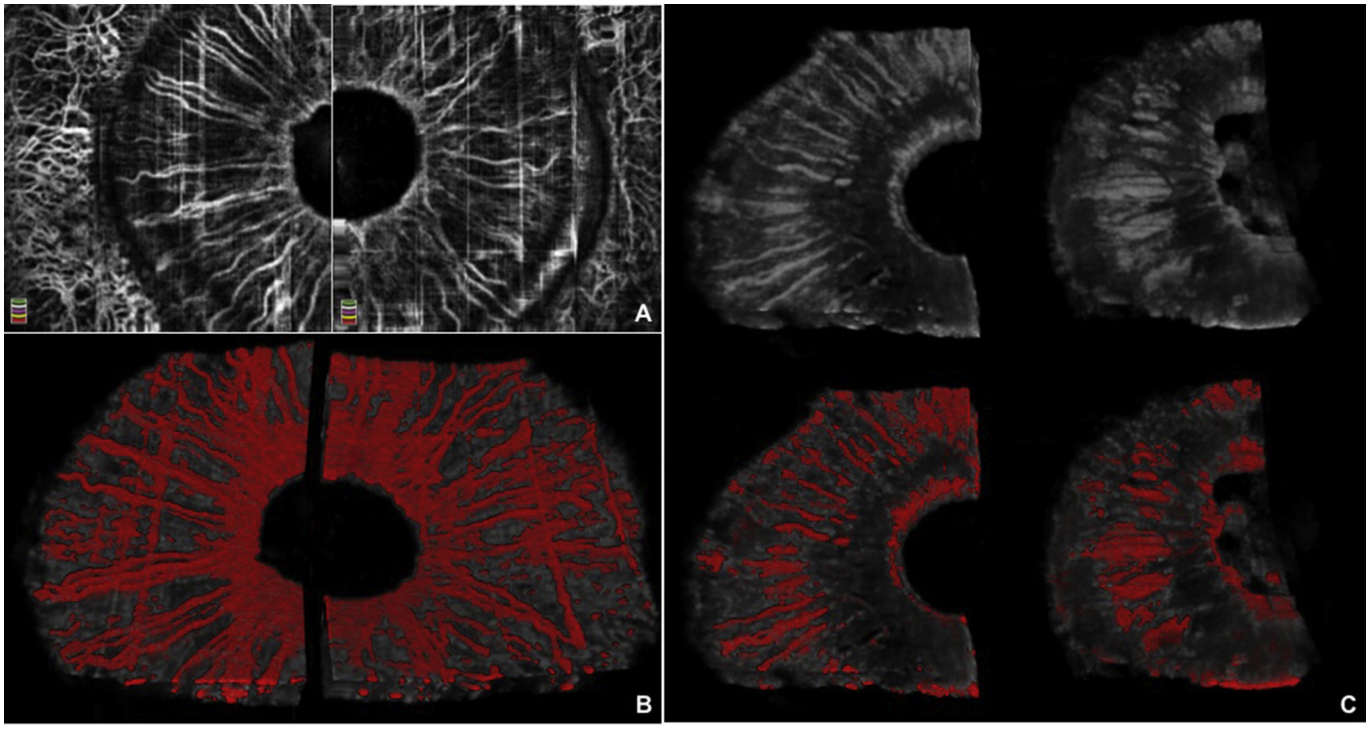

Fig. 4. *Iris vasculature in three anterior uveitis patients with different degrees of anterior chamber inflammation analyzed via OCTA*. Panel A shows a composite of the temporal and nasal OCTA scans of the iris of a patient with anterior uveitis graded as 4 + anterior chamber cells. Through an automated algorithm that creates a 3D rendering of the scans and detect continuous "voxels", vessels segment can be highlighted as in panel B and the volume of their blood flow calculated (0.25 mm^3). The 3D rendering of the irises of two less severe anterior uveitis patients (1 + anterior chamber cells) are shown in the upper portion of panel C, while lower panel highlights the vessels detected through OCTA through an automated algorithm that can as well calculate the volume flow (0.07 and 0.1 mm^3, respectively). OCTA images of the iris (Fig. 3, panel A) are processed using a combination of 3D Gaussian filters, spectral bandpass filters, intensity thresholding and 3D morphological "opening" filters (Fig. 3, panel B) to remove non-specific, non-contiguous voxels and segment bright, connected voxels representing vessel segments (Fig. 3, panel C). Vascular volumes are subsequently calculated by summing voxels in the resulting vessel masks. A mean 3 × 3 vascular iris volume in patients with 4 + anterior chamber cells was 0.28 mm^3, in 3 + cells 0.19, in 2 + cells 0.11, in 1 + cells 0.08 (Fig. 4).

second most common infectious retinal granulomas are the result of ocular toxocariasis (Martínez-Pulgarín et al., 2015), a rare infection caused by roundworms, Toxocara canis and Toxocara cati. Two of the most common ocular manifestations of toxocariasis are posterior pole or peripheral granulomas. The core is formed by the necrotic worm, cellular debris and necrotic eosinophils. This is surrounded by neutrophils, plasma cells, lymphocytes, epithelioid cells and giant cells.

Among the ocular manifestations of cat-scratch disease, a retinal telangiectatic inflammatory mass surrounded by a granulomatous reaction is quite rare.

Intralesional neovascularization can be detected clinically in foci of retinochoroiditis secondary to cat-scratch disease (Mason, 2004) and confirmed with OCTA. In a case recently reported by Pichi et al. (2016b), OCTA highlighted a network of vessels and intralesional microvascular proliferation, (Fig. 5, panel E) not identified with fluorescein angiography (Fig. 5, panel G). In a 12-year-old patient with an active focus of laboratory-proven *Bartonella henselae*, OCTA illustrated a central intralesional feeder vessel, tortuous and fragmented, with circumferential anastomosis and an aspect of pruning of smaller fronds of neovascularization (Fig. 5, panel E). The fact that smaller, physiological capillaries were not visible could be due to their collapse or due to slow flow below the detectable OCTA threshold level. At the 4-month follow-up visit, after a course of full-dose doxycycline, OCTA was repeated and the vascular network density had decreased due to the loss of major anomalous trunks, highlighting the preexisting vessels (Fig. 5, panel F). The Authors comment in the report on the difficulty of correcting the OCTA scan slices for the distorted anatomy caused by the *Bartonella* granuloma and the incapability of distinguishing between dilated abnormal vessels and actual neo-vessels. However, despite these limitations, OCTA is able to highlight better than FA anastomotic vessels inside the granuloma, proving that these vascular lesions may be a feature of retinal *Bartonella* infection (Kostianovsky and Greco, 1994) that can be more frequent than identified with conventional imaging.

The ability to induce endothelial cell proliferation is a common feature of human pathogenic *Bartonella* species (Seubert et al., 2002). This vasoproliferative response may be elicited by vascular endothelial growth factor or migration factors produced either by *B. henselae* or by colonized endothelial cells. *Bartonella* organisms establish an intimate relationship with the vascular endothelium resulting in bacterial adhesion and invasion (Dehio, 2003). These bacterial interactions are directly accompanied by endothelial cell proliferation (Seubert et al., 2002; Dehio, 2003), as well as anti-apoptosis (Dehio, 2003). Bartonella-triggered pathological angiogenesis typically manifests itself systemically in HIV patients either as Kaposi's sarcoma-like lesions of the skin, known as verruga peruana (*B. bacilliformis*) or bacillary angiomatosis (*B. quintana* and *B. henselae*), or as a cystic form in the liver and spleen, referred to as bacillary peliosis (primarily *B. henselae*) (Lax and Thomas, 2002). In the eye, pathological angiogenesis caused by *Bartonella* has been described as peripapillary or macular choroidal neovascularization, but the presence of neovascularization within foci of chorioretinitis has never before been reported. OCTA provides a unique opportunity to detect previously ignored features of pathological disease that may have important mechanistic, diagnostic and treatment implications.

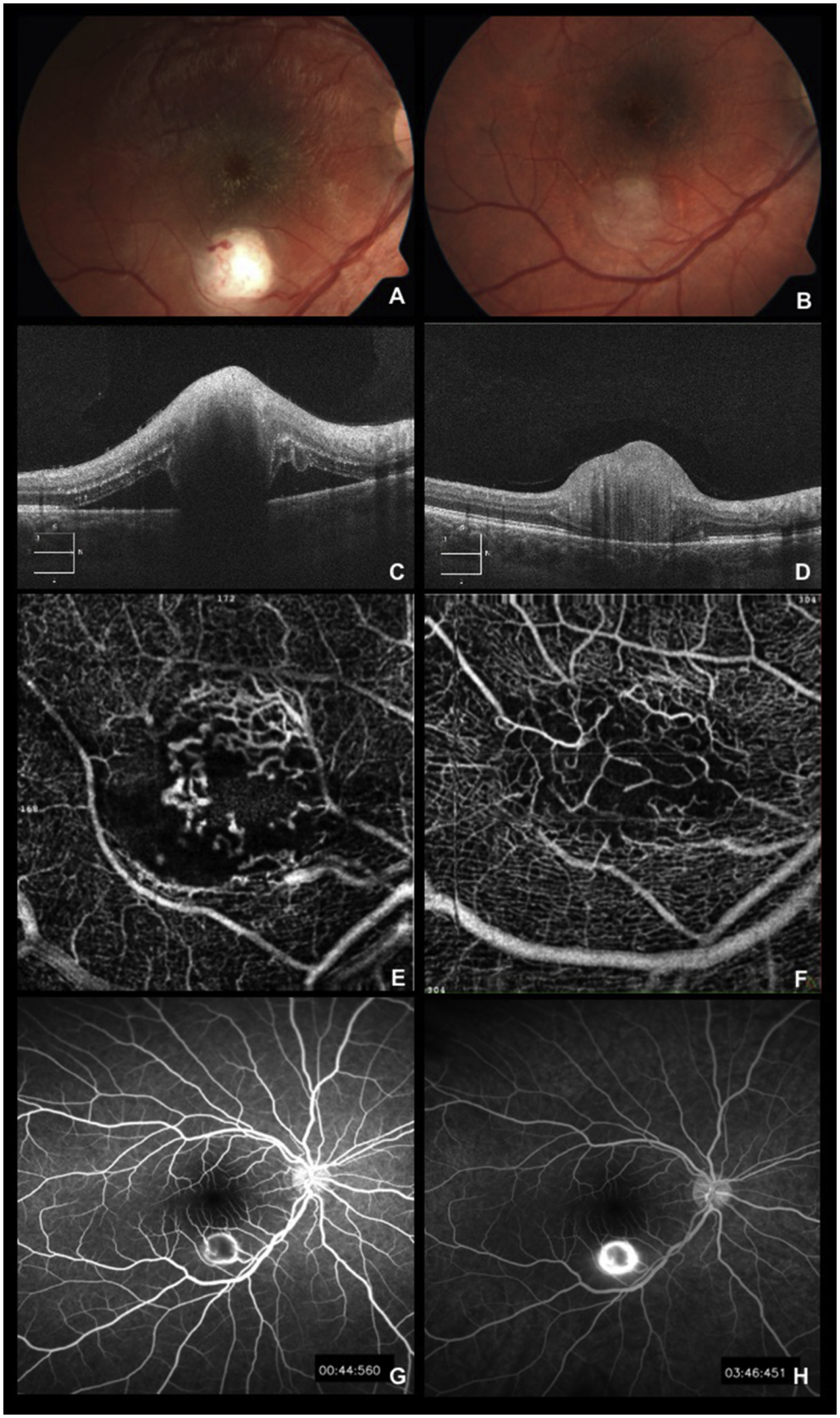

Fig. 5. *Optical coherence tomography angiography highlights anomalous vessels that reside within a Bartonella henselae chorioretinal granuloma.* Color fundus photography of the right eye (A) of a 12-years-old boy with laboratory-proven *Bartonella henselae* chorioretinitis illustrates a white chorioretinal granuloma at the inferior arcade, associated with exudates in a macular star pattern. Anomalous vessels are identified with OCTA on the surface of the infectious granuloma (C). At the last follow-up, the macular exudates have resolved completely and the lesion is noted to be fibrotic (B). Spectral domain OCT of the baseline granuloma demonstrates a hyper-reflective inner retinal lesion with significant shadowing of the outer retina and choroid and associated subretinal fluid (C). Resolution of the shadowing and subretinal fluid is noted with the follow up SD-OCT with increased reflectivity of

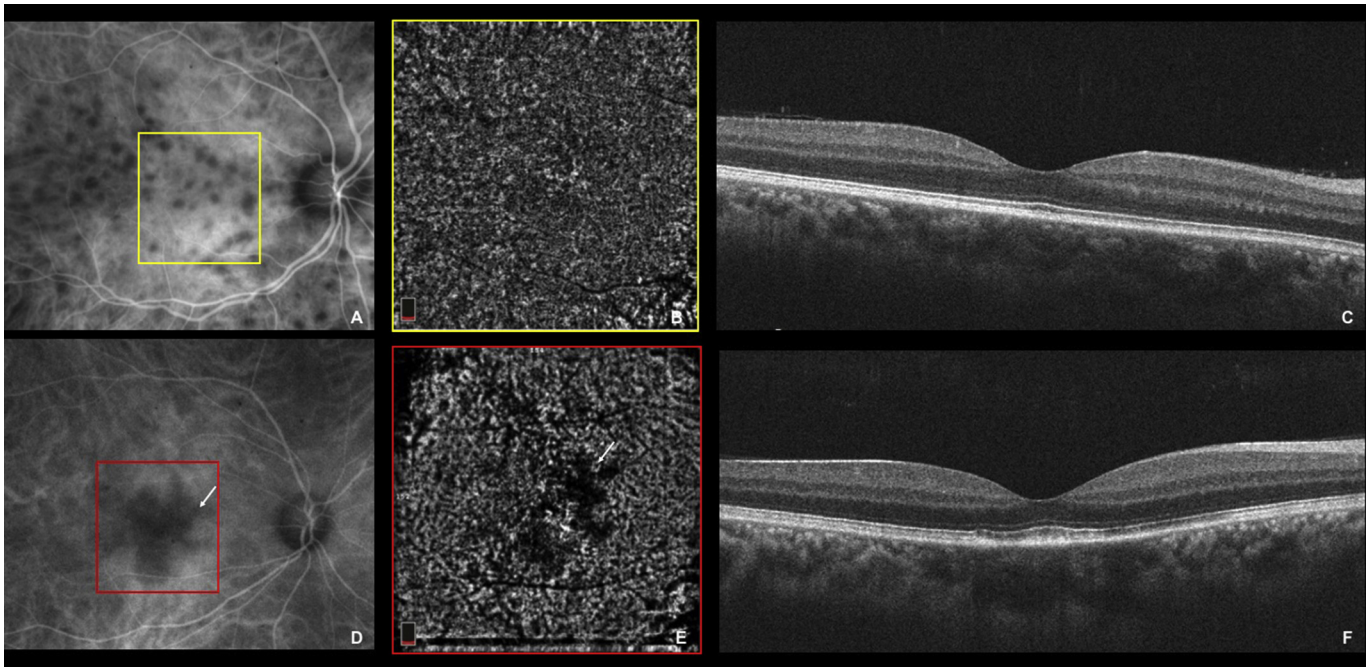

Fig. 6. *Optical coherence tomography angiography in sarcoidosis illustrates intact choroidal flow corresponding to small granulomas and flow void when larger granulomas are present.* The upper panels (A,B,C) illustrate the right eye of a patient with small sarcoid choroidal granulomas that appear as punctate hypofluorescent lesions with indocyanine green angiography (A). These small granulomas are not detected with OCTA at the level of the choriocapillaris (B) or by enhanced depth OCT (C). This may be because smaller granulomas initially grow in the loose connective tissue without alteration of the vascular structure. Their diameter is approximately the size of the lobules of the choriocapillaris, making them indistinguishable with OCT imaging of the choroid. With progressive granuloma growth deeper into the loose choroidal connective tissue, the surrounding vasculature may be shifted and compressed, as illustrated in the bottom panels. Larger choroidal granulomas tend to occupy the full-thickness of the choroid as noted by the choroidal hyporeflectance with EDI-OCT (F), and can be visualized with OCTA as areas of choriocapillaris non-flow (E) that colocalize with ICG hypofluorescence (D).

3.2. Granulomas of the choroid

Granulomatous lesions can affect the choroid either secondary to a systemic granulomatous disease or to a pathologic condition primarily affecting the eye (Mehta et al., 2015).

Sarcoidosis is a disease characterized by the formation of epithelioid cell granulomas in all affected tissues without caseation. An acute onset with erythema nodosum or asymptomatic bilateral hilar lymphadenopathy usually heralds a self-limiting course, whereas an insidious onset, especially with multiple extrapulmonary lesions, may be followed by relentless, progressive fibrosis of the lungs and other organs. Though sarcoidosis is a multisystemic inflammatory disorder, pulmonary manifestations typically dominate (Lynch et al., 1997). The most characteristic finding (present in 50–85% of cases) is bilateral hilar lymphadenopathy (BHL), often with concomitant enlargement of the right paratracheal lymph nodes (Lynch et al., 1997).

Ocular involvement is seen in a significant number of patients with sarcoidosis. Yellow-grey nodular lesions may appear in the choroid or outer retina (Gass and Olson, 1976) and these sarcoid-associated granulomatous uveitis can cause visual disability from inflammatory sequelae such as physical distortion and edema of the overlying retina (Papavasileiou et al., 2016), and in some extreme cases chorioretinal ischemia (Invernizzi et al., 2015).

Small sarcoid granulomas tend to be localized to the inner choroidal stroma since leukocyte diapedesis starts in Sattler's layer (Invernizzi et al., 2015) (Fig. 6, panel C) where blood vessels have thinner walls and demonstrate punctate hypofluorescence with ICGA (Fig. 6, panel A). Their diameter approximately corresponds to the size of the choriocapillaris (Invernizzi et al., 2015) lobules but are not identified with OCTA due to low flow (Fig. 6, panel B). The inflammatory cells initially expand by infiltrating the loose connective tissue between the vascular structures and causing a granulomatous choroidal arteriolitis (Chen and Xu, 2013). Since each choroidal lobule is supplied by a single arteriole, choroidal arteriolitis affects choroidal circulation by the lobular unit (Mehta et al., 2015). As the granulomas grow, they extend in the loose choroidal connective tissue (Fig. 6 panel F) and shift and compress the surrounding vasculature (Chen and Xu, 2013). Larger, full thickness choroidal granulomas can be visualized on OCTA (Fig. 6, panel E) as areas of choriocapillaris non-flow that co-localizes with the ICG hypofluorescent lesions (Fig. 6, panel D).

4. Optical coherence tomography angiography of the superficial retinal capillary plexus in uveitis

Qualitative and quantitative abnormalities in the density and morphology of the parafoveal retinal capillary plexus of subjects with uveitis have recently been described in a number of OCTA studies (Agarwal et al., 2016; Aggarwal et al., 2016; Cerquaglia et al., 2016; Klufas et al., 2017; Phasukkijwatana et al., 2016; Salvatore et al., 2016). Assessment of the foveal microvasculature using fluorescein angiography (FA) is limited by the trilaminar or triplanar pattern of the capillary networks (Park et al., 2016) and by

the granuloma associated with residual disorganization of the inner retinal layers (D). The anomalous vessels are highlighted with OCTA at the level of the deep capillary plexus. Note the pruning of vessels at the core (E). Follow up OCTA illustrates significant resolution of the anomalous vessels and restoration of the normal deep retinal capillary plexus (F). Fluorescein angiography was not effective in highlighting the vascular nature of the lesion. Early frames (G) illustrated hyperfluorescence of the lesion margins while later frames (H) demonstrated pooling within the entire lesion.

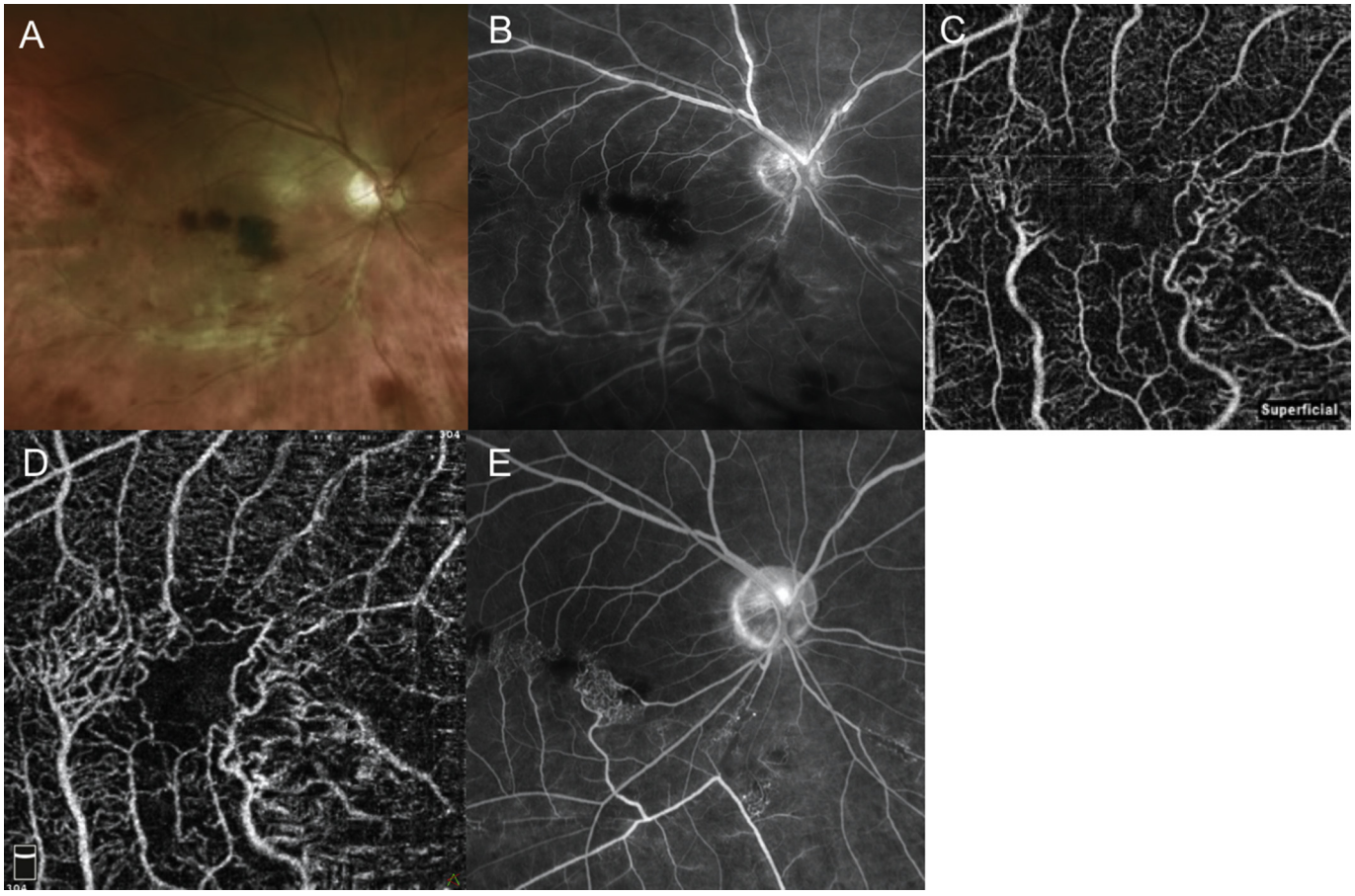

Fig. 7. *Microvascular Remodeling in Idiopathic Retinal Vasculitis.* A 59-year-old man with idiopathic retinal vasculitis and panuveitis of the right eye presents during an active recurrence of disease. (A) Optos color photograph of the right eye illustrates retinal hemorrhage in the macula and sheathing along the inferotemporal arcade. (B) Optos FA demonstrates blockage from the hemorrhage and inferior vascular tortuosity. OCTA of the superficial retinal capillary plexus at the same visit (C) illustrates microvascular remodeling and microaneurysms in greater detail than identified with FA. OCTA 3 months later (D) after treatment demonstrates the collaterals more clearly with resolution of the hemorrhages. FA obtained 8 months after the acute flare (E) highlights the capillary remodeling identified with OCTA, but the microvascular details such as the presence of inferior capillary nonperfusion (i.e. flow deficit) are partially masked by background hyperfluorescence.

leakage. In particular, FA has poor resolution of the deep retinal capillary plexus (Nemiroff et al., 2016; Weinhaus et al., 1995). Furthermore, other factors may limit the visualization of the capillary network with FA including media opacities (e.g. cataract), absent early frames of the study and obstruction from macular edema and dye leakage. Optical coherence tomography angiography provides high-resolution images with depth resolved visualization of both the superficial and deep retinal capillary plexus and detection of microvascular abnormalities that are not identified using fluorescein angiography.

4.1. Inflammatory vasculitis

Vasculitis is considered a specific disorder in which components of the blood vessels are the center of the inflammatory focus. The retinal vessels may be involved in almost all forms of intermediate and posterior uveitis. The precise pathological definition restricts the term vasculitis to the appearance of direct damage and infiltration of the vessel wall by inflammatory cells. In part this definition is based on the concept that the endothelial cell is the primary target of attack. Molecular, cell biological and clinical evidence supports the notion of an endothelial cell-specific immune disease.

Retinal vasculitis may manifest with blurring or loss of vision, floaters or scotoma. It may be asymptomatic, particularly when it is located in the peripheral retina and not associated with vitritis. A sudden decrease of vision due to vitreous hemorrhage may reveal retinal vasculitis in some patients. Ocular symptoms may be uni- or bilateral. Active vasculitis is characterized by focal, multifocal or diffuse fluffy white sheathing or cuffing of blood vessels. Pathological sheathing is revealed to be due to perivascular infiltration of inflammatory cells, which can be quite variable in extent, and produces the conical visible blurred vessel margins. In the later stages, the affected vessels show well-defined gliotic sheathing (El-Asrar et al., 2010). Other vascular changes that may accompany retinal vasculitis include telangiectasis, vascular anastomoses, microaneurysms, macroaneurysms and optic disc or preretinal neovascularization.

The challenge in evaluating patients with retinal vasculitis relates to the heterogeneity of the disease and the need to determine when and to what extent a patient has “active” inflammation of the retinal vessels wall (Park et al., 2016). FA is more sensitive than clinical examination in the diagnosis of retinal vasculitis, showing staining of the blood vessel wall and leakage. Capillaritis, characterized by capillary leakage and areas of capillary non-perfusion, can be detectable only by FA (Walton and Ashmore, 2003). However, leakage of dye can limit our ability to evaluate adjacent capillary perfusion (Fig. 7, panel A and B). Moreover, leakage can be present due to previously damaged or ischemic capillary beds in the absence of active inflammation (Fig. 7, panel E). OCTA is not

limited by leakage (or other causes of hyperfluorescence on FA such as pooling and window defect), and can provide microvascular morphological detail and information regarding capillary perfusion, with quantitative capability, of both the superficial and deep capillary plexus (Leder et al., 2013; Lee and Rosen, 2016).

Employing a prototype SD-OCTA device (Cirrus, Carl Zeiss Meditec, Inc., Dublin, CA, USA), Kim et al. (2016) attempted to distinguish the differences in macular capillary density or morphology between 61 uveitic and 94 healthy eyes. The authors performed a cross-sectional OCTA analysis of 61 eyes, imaged with intensity (i.e. amplitude)-only (Group 1) or a combined intensity (i.e. amplitude) and phase-based algorithm (Group 2) associated with semi-automated segmentation of the retinal capillary layers, or with combined intensity and phase-based algorithm and manual segmentation (Group 3). The superficial capillary plexus was automatically calculated as 60% of the depth between the inner limiting membrane and 110 μm above the retinal pigment epithelium. Of these 61 eyes, 28 eyes had retinal vasculitis. A significantly lower parafoveal capillary density was illustrated in the superficial retinal plexus of uveitic compared to healthy eyes. Uveitic subjects also demonstrated significantly lower branching complexity in the superficial retinal capillary plexus. Vessel diameter was not significantly different in either layer. The differences identified between healthy and uveitic eyes were consistent and significant whether they were identified by semi-automated (Groups 1 and 2) or manual (Group 3) segmentation methods to define retinal layer boundaries, and whether an intensity only (Group 1) or intensity and phase (Groups 2 and 3) based OCTA was employed.

Bessette et al. (2016) employed 3 × 3 mm and 6 × 6 mm OCTA (Avanti RTVue-XR, Optovue Inc., Fremont, CA) in 26 patients (52 eyes) with retinal vasculitis. Abnormalities subjectively identified on OCTA were similar to the study by Kim et al. (2016) and included capillary dropout or loss in the superficial retinal capillary plexus (Fig. 7, panel C), enlargement and/or irregularity of the foveal avascular zone, capillary remodeling, and normal flow in the presence of exudates. The average flow density (3 × 3 mm scan) of the superficial retinal capillary plexus was 49.63 ± 4.84%. In patients without involvement of the macula, defined as leakage within the vascular arcades on fluorescein angiography, the average flow density in the superficial plexus was 51.12 ± 4.60%. In patients with involvement of the macula, the superficial flow density was 47.48 ± 4.37%. The differences between eyes with and without involvement of the macula were statistically significant ($p = 0.01$). Bessette et al. (2016) further demonstrated that the difference

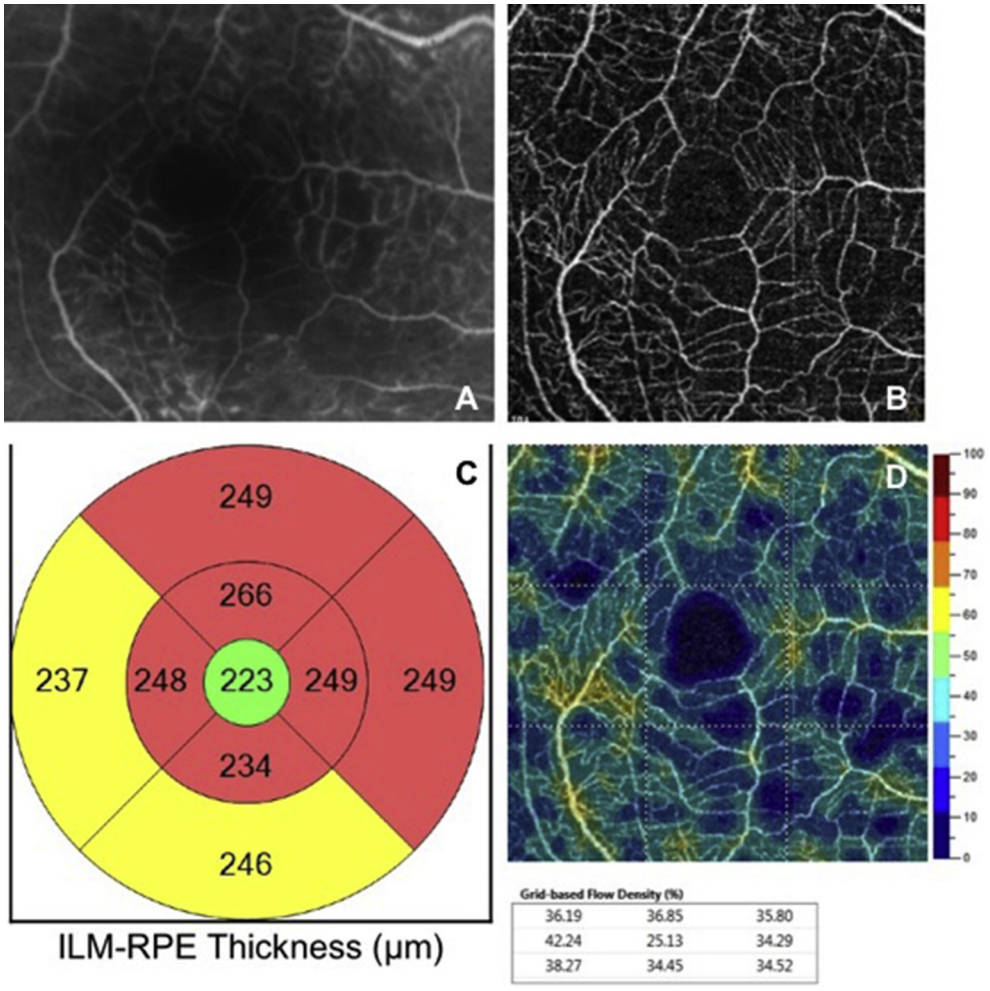

Fig. 8. *In symptomatic birdshot chorioretinopathy patients who are clinically inactive, OCTA illustrates perifoveal ischemia.* This 48-year-old woman was diagnosed with birdshot chorioretinopathy 8 years prior. After treatment with mycophenolate mophetil (2 g for the prior 2 years), she was considered clinically inactive. Patient's visual acuity was 20/20 in the right eye but she complained of photopsia and shimmering vision. With fluorescein angiography (A) no leakage is detected in the macular region, but a rarefaction of the capillaries with telagiectatic loops is noted. Optical coherence tomography angiography of the superficial plexus highlights more accurately the diffuse perifoveal areas of capillary non-flow (B). Central retinal thickness may be decreased in long-standing birdshot chorioretinopathy, and in this case thinner areas in red on the OCT map (C) co-localize to the color-coded OCTA map of non-perfusion (D), where color blue corresponds to areas of non-flow.

between eyes with and without involvement of the macula was not statistically significant at the superficial capillary levels for the 6 × 6 OCTA scans when comparing all eyes (p = 0.10) or when comparing eyes with macula involvement to their fellow, uninvolved eyes.

Given that vascular leakage is not identified with OCTA, it is possible that fluorescein angiography may be more sensitive in determining when a patient is active. In the study by Bessette et al. (2016), only 56% of eyes that were active, with activity defined as leakage of the dye from the vessels on fluorescein angiography, illustrated abnormalities on OCTA. On the other hand, 13 patients demonstrated changes in the retinal microvasculature on OCTA that were not identified with FA. In patients who had reperfusion of a prior branch retinal artery occlusion, for example, capillary dropout was more easily identified with OCTA compared to FA and, in some cases, not even visible with FA. As such, the absence of vascular leakage with OCTA can be advantageous as hyperfluorescence due to vascular leakage or window defects may impede the detection of capillary perfusion.

Despite its limitations in demonstrating active inflammation, OCTA may be more useful than FA in quantifying progressive capillary loss in the macula due to prior episodes of retinal vasculitis. This information can have important implications as the clinician may consider the area of capillary reserve in order to guide treatment decisions for the patient.

4.2. Birdshot chorioretinopathy (BSCR)

Birdshot chorioretinopathy (BSCR) is a form of inflammatory posterior uveitis with a distinct clinical phenotype consisting of mild anterior uveitis, moderate vitritis, retinal vasculitis and numerous oval creamy white choroidal lesions scattered throughout the fundus that appear like birdshot from a shotgun. Hence, the term birdshot chorioretinopathy was introduced by Ryan and Maumenee in 1981. In 2006, research criteria for BSCR were published based on the consensus of an international panel. Imaging findings are not well defined in the 2006 classification scheme (Levinson et al., 2006), mostly because of the lack of correspondence between the various imaging techniques. While in most chorioretinal inflammatory diseases the inflammatory process takes place in one structure with contiguous extension, in BSCR the pathogenesis of inflammation occurs independently, but simultaneously, in the choroid and the retina. Due to the progressive nature of BSCR, it is essential to have accurate methods of monitoring disease activity and measuring tissue damage. BSCR may in fact demonstrate a long insidious course (Touhami et al., 2016), and studies have demonstrated a progressive deterioration of both central and peripheral retinal function (Symes et al., 2015), even in the absence of clinically detectable inflammation (Jack et al., 2016). If undertreated, chronic inflammation may lead to retinal atrophy and a retinitis pigmentosa-like degeneration may even occur (Symes et al., 2015; Touhami et al., 2016). Snellen visual acuity is a notoriously imprecise indicator of visual function and progression of inflammation in BSCR and therefore alternative biomarkers are employed to monitor disease activity and guide treatment including formal visual field analysis and full field electroretinography (Cao et al., 2016; Minos et al., 2016).

de Carlo et al. (2015) studied a total of eight eyes of four patients with birdshot chorioretinopathy with optical coherence tomography angiography (OCTA). OCTA of the superficial retinal capillary plexus was evaluated using a segmentation slab between the internal limiting membrane and Bruch membrane and microvascular abnormalities were assessed in the posterior pole. Abnormal telangiectatic vessels were observed in all 8 eyes (100%) with birdshot chorioretinopathy. Capillary dilatations and loops were each identified in 7 of the 8 eyes (88%). Increased intercapillary space was demonstrated in all 8 eyes (100%) and was diffusely distributed throughout the posterior pole and most prominent temporally in 6 of the 8 eyes (75%) and noted focally in 2 of the 8 eyes (25%).

Pichi et al. (2016c) employed OCTA to evaluate 44 BSCR eyes (22 patients, mean age 41 years, range 31–64) that were deemed inactive on imaging (OCT and FA) and clinical exam (based on Standardization of Uveitis Nomenclature criteria) (Jabs et al., 2005). The mean best corrected visual acuity at the enrollment visit was 0.01 ± 0.1 logMAR (20/20 Snellen equivalent) and at the 12 months follow-up was 0.13 ± 0.25 logMAR (20/25 Snellen equivalent) (P was non-significant at 0.1).

The early frame FA (cropped) Fig. 8, panel A) was compared to the 3 × 3-mm OCTA segmented at the level of the superficial retinal capillary plexus (Fig. 8, panel B),. The FAZ and the area of capillary non-perfusion were manually outlined and measured (Hartig, 2013) by 2 examiners using ImageJ (http://imagej.nih.gov/ij/; provided in the public domain by the National Institute of Health, Bethesda, MD, USA). In their series, the FAZ of birdshot patients was more precisely identified with OCTA providing better delineation of the area and better detection of enlargement versus FA. The FAZ mean area manually measured on the 3 × 3 mm OCTA images was larger in eyes with BSCR (1.34 ± 0.41 mm^2; $P < 0.0001$) compared to data reported in literature on normal healthy eyes.

The most noticeable abnormality in the retinal vasculature was increased perifoveal intercapillary spaces in all BCR eyes. These areas of perifoveal ischemia were reliably measured manually at the level of the superficial capillary plexus with OCTA, with a good interobserver agreement (mean 0.9 ± 1.2 mm^2, κ 0.82). However, there was only moderate agreement regarding evaluation of ischemic areas using conventional FA (κ of 0.22). In their study, perifoveal areas of ischemia in BSCR were also measured automatically using the color-coded topographic perfusion density map (mean 0.97 ± 0.03)When the automated flow indices were decreased with OCTA, suggestive of ischemia, this correlated with a greater severity of disease in a statistically significant fashion.

Vascular changes in the SCP with OCTA, in long-standing BSCR patients, may indicate actual areas of ischemia or non perfusion, or may be secondary to reduced flow within the superficial parafoveal circulation. Split-spectrum amplitude-decorrelation angiography employs a threshold of flow detection and is not enable to detect retinal capillary flow outside the range of 0.3 mm/s to 2 mm/s. Therefore, the blood flow in the superficial capillary plexus may be barely detectable using the split-spectrum amplitude-decorrelation angiography algorithm (Spaide et al, 2015a). This would fit well with the assumption that BSCR could cause hypoperfusion of the superficial capillary plexus, resulting in tissue hypoxia and possible cellular death.

Furthermore, OCTA findings were compared to central retinal thickness (CRT) as measured by SD-OCT. Areas with decreased capillary perfusion on OCTA illustrated a statistically significant correlation or co-localization with areas of decreased CRT with SD-OCT ($P < 0.001$) (Fig. 8, panel C). It is intriguing to speculate whether flow reduction may be associated with ischemia that could lead to a decrease of retinal thickness on SD-OCT. Previous studies have demonstrated that anatomic macular thinning is associated with long-term birdshot retinochoroidopathy (Silpa-Archa et al., 2016), and have provided direct evidence that the major cause of macular thinning in birdshot is thinning of the outer retina. However, the superficial retinal capillary plexus is located predominantly within the ganglion cell layer, which has a high oxygen demand. Due to the greater metabolic demand, the region

of the parafoveal capillary plexus may be at higher risk of ischemic insult (Lee and Rosen, 2016; Park et al., 2016). Therefore, it could be possible that a major contribution in BSCR macular thinning comes from an ischemic insult to ganglion cells and their axons.

5. Optical coherence tomography angiography of the deep retinal capillary plexus in uveitis

The deep retinal capillary plexus (DCP) has a vortex-like and less-continuous pattern of vessels consistent with the fact that capillaries in this segment are diving into and out of the plane of the image (Gorczynska et al., 2016; Spaide et al, 2015a). The DCP with OCTA consists of both the true decorrelation signal from blood flow within that layer and the projection artifacts from the SCP (Spaide et al, 2015a).

5.1. Inflammatory vasculitis

In the study by Kim et al. (2016), the deep retinal capillary plexus (DCP) in the 28 patients with retinal vasculitis was automatically assessed as the remaining 40% of the depth with an automated segmentation up to 110 μm above the RPE. The DCP on OCTA illustrated smaller magnitudes of changes for vessel density and diameter, compared to the sloped magnitudes of change when comparing the SCP of healthy eyes versus uveitic eyes. This smaller magnitude of change in the deep retinal plexus may be attributed to the confounding effects of projection artifacts that may impede detection of real but small changes at this level. The authors used a manual segmentation methodology to correct for projection artifacts from the SCP by selecting only for perfusion within the DCP and deriving the angiogram from this raw OCT B-scan flow data. While this correction method was not standardized, the larger magnitudes of change in the deep retinal layer of group 3 (manual segmentation method) compared to groups 1 or 2 (semi-automated segmentation method) suggest that OCT angiographic vascular changes of the DCP may be underestimated due to projection artifacts.

Bessette et al. (2016) performed an automated quantitative flow density analysis of the DCP using 3 × 3 mm and 6 × 6 mm scans in their cohort of vasculitis patients. DCP Flow density was compared between eyes with and without clinical involvement of the macula on fluorescein angiography (Fig. 7, panel D and E). The average flow density (3 × 3 mm scan) of the deep plexus was 54.46 ± 5.02 %In patients without macular involvement, the average flow density in the deep plexus was 56.66 ± 3.76%.In patients with involvement of the macula, it was 51.27 ± 4.91%. The differences between eyes with and without involvement of the macula were statistically significant for the DCP ($p = 0.0006$). More important, compared to the superficial plexus, Bessette et al. (2016) noticed only minor ischemic abnormalities in the deep plexus of vasculitic eyes on OCTA. This finding may be in discordance with that reported in the literature regarding the deep plexus, in eyes with retinal vascular disease or retinal vascular occlusion (Nemiroff et al., 2016). The DCP may be more prone to ischemia as it is positioned in a watershed-like region, compared to the superficial plexus. However, in their analysis, Bessette et al. (2016) did not address the projection artifacts identified at the level of the DCP from the vessels above. It is possible that if the SCP was subtracted from the DCP in their measurements, a greater extent of ischemia would be noted.

5.2. Uveitic macular edema

The term “cystoid macular edema” describes an accumulation of intraretinal fluid, normally located in the fovea region. It represents a common and serious complication of uveitis that may incur a long-ranging negative impact on a patient's quality of life. It has been estimated that cystoid macular edema (CME) is responsible for 40–50% of cases of irreversible visual impairment in uveitis (Lardenoye et al 2006). However, not all patients with uveitis are at the same risk to develop this complication. In a cross-sectional study on 529 uveitis patients performed by Lardenoye et al., in 2006, 33% of patients presented with CME in at least one eye. In their study there was a clear relationship between the occurrence of CME and the anatomic type of uveitis. Panuveitis was the leading association with 66% of patients presenting with CME, followed by intermediate uveitis (60%), posterior uveitis (34%), scleritis (13%), and anterior uveitis (11%). The authors also found a clear correlation between specific uveitis entities and the frequency of CME. Those uveitis entities complicated by CME in more than 50% of patients included sarcoidosis (59%), juvenile idiopathic arthritis (60%), Behçet's disease (63%), birdshot chorioretinopathy (100%), and acute retinal necrosis (100%).

The exact pathophysiology of CME in intraocular inflammation remains unclear. Basically, the integrity of the blood–retinal barrier is responsible to maintain the stability of the environment of ocular neurons and photoreceptors (Guex-Crosier, 1999). The blood–retinal barrier is maintained at two levels: tight junctions in the retinal pigment epithelium form an outer barrier, whereas tight junctions between the endothelial cells of retinal vessels form an inner barrier (Cunha-Vaz, 1979; Raviola, 1977). Various inflammatory mediators such as prostaglandins, interleukins (e.g., IL-1, IL-2, IL-10), interferon gamma, and tumor necrosis factor alpha induce a break-down of the blood–retinal barrier that leads to an influx of fluid from vessels into or under the retinal tissue resulting in extracellular edema (Rotsos and Moschos, 2008; Wakefield and Lloyd, 1992). However, a breakdown of the blood–retinal barrier is probably not the only possible pathomechanism of CME. It has also been postulated that swelling of Müller glia cells may contribute to the development of CME. Intracellular fluid accumulation in the absence of vascular leakage with fluorescein angiography, results in cysts formed by swollen and dying Müller cells (Bringmann et al., 2004; Yanoff et al., 1984).

Funduscopy is not always a sensitive method to detect CME and to differentiate it from other exudative maculopathies, however spectral domain OCT offers important advantages. As a noninvasive method, it can be repeated as often as necessary. Furthermore, OCT can locate the level and map the distribution of fluid and provide biomarkers of quantification including retinal thickness (Tran et al., 2008). This makes it an optimal tool for follow-up of uveitic CME and assessment of treatment response. In a prospective comparative observational series by Antcliff et al. (2000) OCT demonstrated a sensitivity and specificity for detecting uveitic CME of 96 and 100%, respectively, compared with FA. Using OCT, Markomichelakis et al. (2004) identified three different patterns of uveitic macular edema: (1) diffuse macular edema “characterized by increased retinal thickness, disturbance of the layered retinal structure, or sponge-like low reflectivity areas”; (2) cystoid macular edema “characterized by the formation of clearly defined intraretinal cystoid spaces”; and (3) serous retinal detachment which is “characterized by a clean separation of the neurosensory retina from the retinal pigment epithelium/choriocapillaris band.” Sivaprasad et al. (2007) made further differentiation whether cysts are located in the inner or outer layer of the retina. These studies were however limited by the use of time domain OCT.

Kim et al. (2016) performed a quantitative OCTA analysis on eyes with macular edema to determine whether its presence was associated with alterations in DCP density or morphology. In their cohort of uveitis patients, 16 eyes had macular edema. Analysis

revealed significantly lower vessel density in the deep plexus of uveitic subjects with macular edema ($P < 0.001$). No significant differences were found in the superficial plexus. These significant changes in the deep capillary plexus parameters co-localized with the location of intraretinal cystoid spaces in the inner retina (generally inner nuclear and plexiform layers) in their analysis, and thus the authors did not attribute them to any potential projection artifacts. While these findings could be explained by segmentation and projection artifact created by the cystoid spaces that can alter the reliability and accuracy of DCP OCTA analysis, Spaide et al., (2015b) has noted that DCP ischemia may be an important driving mechanism in the development of CME in retinal vascular disease such as diabetic retinopathy.

5.3. Birdshot chorioretinopathy

Phasukkijwatana et al. (2016) were the first to analyze the deep capillary plexus in a patient with birdshot chorioretinopathy. The authors describe a patient with a 6 years history of BSCR, associated with vitreous hemorrhage and retinal neovascularization, treated with mycophenolate mofetil and multiple off-label bevacizumab injections. An analysis of the vessel density on OCTA of the superficial and deep plexus demonstrated diffuse reduction of flow that was more profound in the deep compared to the superficial capillary plexus. Their finding of more significant flow reduction at the deep capillary plexus level with OCTA may indicate that ischemia, in addition to inflammation, may play a role in the development of complications such as retinal neovascularization in BSCR.

Most importantly, the case by Phasukkijwatana et al. (2016) highlights the importance of understanding projection artifacts at the deep capillary level. To deal with this problem, the authors positioned the segmentation slab slightly posterior to the DCP and subtracted the superficial plexus by using ImageJ. While this method removes the artifacts from above, it may be responsible for a partial signal loss of the true DCP and has not been validated. Once again, the future development of OCTA algorithms to remove projection artifact would be a major advancement for this imaging modality.

6. Optical coherence tomography angiography of choroidal neovascularization in uveitis

6.1. Inflammatory choroidal neovascular membranes

Inflammatory choroidal neovascularization is a potential complication of uveitis often resulting in severe vision loss. Its pathophysiology remains poorly understood, partially due to the lack of a strong animal model, limited to laser-induced CNVs (Shah et al., 2015). Nevertheless, a series of pathophysiological pathways have been suggested. It has been proposed for example, that inflammation-induced disruption of Bruch's membrane and/or the outer retinal barrier can be associated with ischemia which can drive the choroid to produce vascular endothelial growth factor (VEGF) (Forrester et al., 1990; Parvan and Margo, 1996). In addition to VEGF, inflammatory mediators are widely thought to be involved in the development of choroidal neovascularization even in non-inflammatory diseases, and these mediators may also participate in the development of uveitic choroidal neovascularization (Espinosa-Heidmann et al., 2003; Forrester et al., 1990; Parvan and Margo, 1996).

Early recognition of inflammatory choroidal neovascularization is critical for timely and appropriate therapy and to avoid permanent visual impairment. Although the gold standard for the diagnosis and management of inflammatory choroidal neovascularization is dye-based angiography, interpretation of dye-based tests may be limited by the similarities between purely inflammatory lesions versus neovascularization. Traditional OCT has been widely used as an adjunct to dye based tests for the clinical assessment of such disease and is a valid tool for the multimodal evaluation of this complication of uveitis (Onal et al., 2014).

With the introduction of OCTA, some reports have studied the clinical OCTA findings of inflammatory choroidal neovascularization. Inflammatory choroidal neovascularization is characterized by yellow-white lesions associated with retinal thickening and on occasion subretinal blood. Fluorescein angiography demonstrates a hyperfluorescent area that leaks during the late phases of the angiogram. Chorioretinal inflammatory lesions can be confused with inflammatory choroidal neovascularization, since the leakage can be a hallmark of both lesion types (Watzke et al., 1984). Traditional OCT scans may reveal subretinal hyperreflective tissue (nonspecifically referred to as SHRM or subretinal hyperreflective material) that can be consistent with type 2 neovascularization, but this is not a universal finding of CNV activity and the lesion (SHRM) can represent other abnormalities such as subretinal fibrin or fibrosis.

By contrast, 3×3 mm OCTA can identify a neovascular network in the subretinal (type 2) or subRPE (type 1) compartment, confirming the presence of CNV. The area and the density of the inflammatory CNV can be quantitated. It is possible OCTA will provide a more precise and practical means of evaluating for inflammatory choroidal neovascularization versus dye-based modalities.

6.1.1. Inflammatory choroidal neovascular membranes in acute zonal occult outer retinopathy

The first case of inflammatory choroidal neovascularization secondary to AZOOR studied by OCTA was reported by Levison et al. (2016a). The authors described a 74-year-old female with acute zonal occult outer retinopathy who presented with a subretinal lesion suggestive of inflammatory choroidal neovascularization. Optical coherence tomography angiography confirmed the presence of a neovascular lesion and supported the management of this complication.

6.1.2. Inflammatory choroidal neovascularization in punctate inner choroidopathy

Punctate inner choroidopathy (PIC) is a rare, idiopathic, inflammatory disease confined to the inner choroid and retinal pigment epithelium that occurs in otherwise healthy, predominantly young adult myopic women. PIC was first described in a cohort of ten women (Watzke et al., 1984). An important distinguishing feature of PIC is the absence of anterior chamber or vitreous inflammation (Watzke, 1984). The funduscopic examination is characterized by multiple punctate yellow-to-white inflammatory lesions, measuring 100–300 μm at the level of the retinal pigment epithelium and the inner choroid, which may eventually become atrophic, pigmented scars. These lesions characteristically cluster in the posterior pole and are generally not found in the peripheral retina. The most important vision-threatening complication of PIC is choroidal neovascularization (CNV), which may be present on the exam (Gerstenblith, 2007).

The OCTA findings observed in patients with punctate inner choroidopathy (PIC) complicated by inflammatory choroidal neovascularization were recently described (Levison et al., 2016b) in a prospective, descriptive case series of 12 patients including 7 patients with PIC complicated by inflammatory choroidal neovascularization. Inflammatory choroidal neovascularization was identified in 11 of the 12 patients (15 eyes). Optical coherence tomography angiography detected inflammatory choroidal

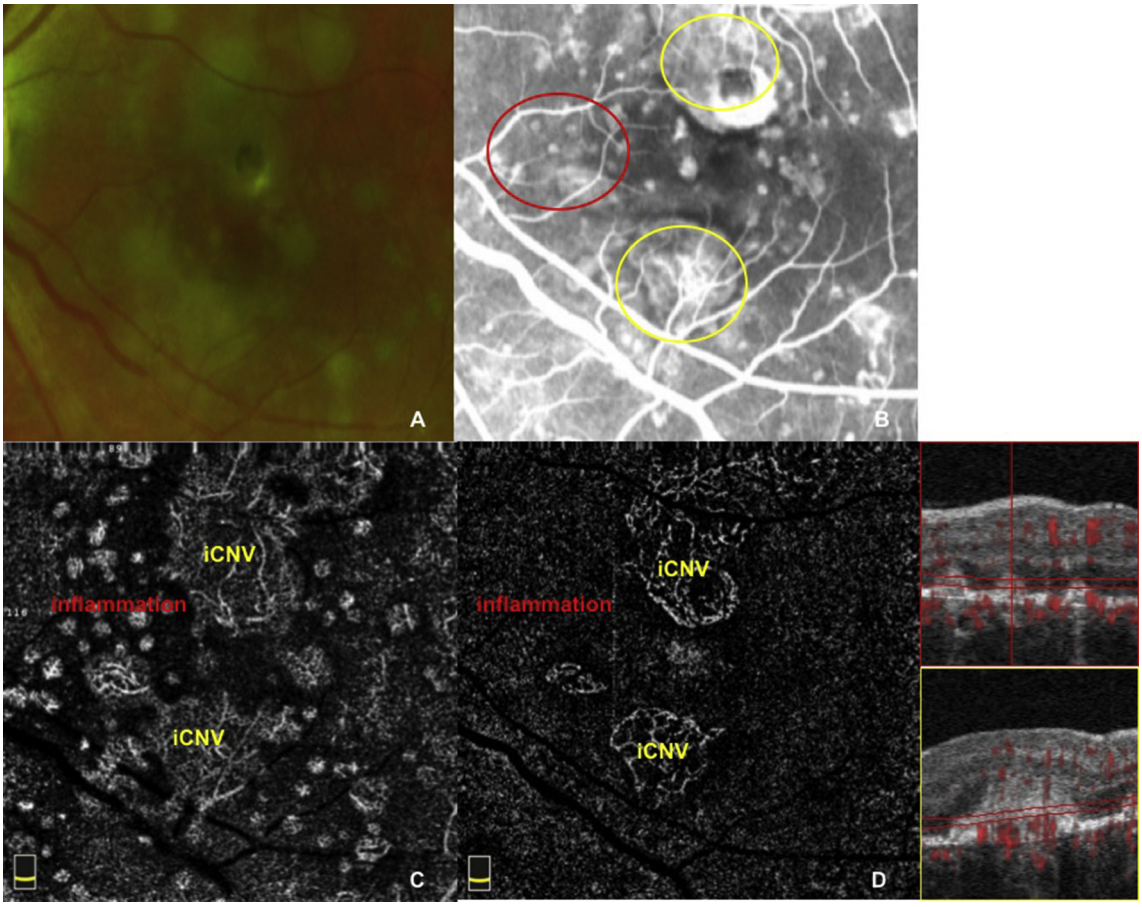

Fig. 9. *Optical coherence tomography angiography of a patient with active multifocal choroiditis may be helpful in distinguishing purely inflammatory lesions from inflammatory choroidal neovascularization.* Multiple white-yellow dots in the macula of a 27-year-old white female with multifocal choroiditis (A) correspond to hyperfluorescent areas on FA (B), some smaller and round (red circle) and some suspicious of predominantly classic choroidal neovascular membranes (yellow circles). A 3 × 3-mm OCT angiogram at the level of the ellipsoid zone (C) demonstrated 2 different kind of lesions: diffuse, small, round lesions with an associated network of vessels inside (red); and larger, confluent lesions consisting mainly of lacy vessels (yellow). The small round lesions corresponded to conical RPE elevations (red square), and were absent in the outer retina OCTA scan (D), indicating that the associated vessels were likely due to projection artifact. The larger lesions illustrated a lacy networks of vessels (yellow) visible even in the outer retina scan (D), confirming their truly vascular nature, most likely consisting of iCNV.

neovascularization when the traditional dye test failed to clearly identify the neovascular lesion. Optical coherence tomography angiography was also very informative regarding the follow-up assessment and treatment response of the CNV microstructure. With anti-vascular endothelial growth factor (VEGF) treatment there was a trend towards larger, more distinct vessels, suggesting CNV maturation (Kuehlewein et al., 2015), although the lesions were not treatment-naïve at baseline. The authors also noted an associated ring of hyporeflectivity around the CNV identified by OCTA, that increased in size in certain cases suggestive of neovascular activity.

6.1.3. Inflammatory choroidal neovascular membranes in multifocal choroiditis

Multifocal choroiditis (MFC) was first described in 1973 (Michel et al., 2002) with chorioretinal findings resembling ocular histoplasmosis syndrome. The first series of patients was reported in 1984 (Dreyer and Gass, 1984) with lesions primarily at the level of the RPE and inner choroid associated with vitreous cells, and the syndrome was named multifocal choroiditis with panuveitis but the cause of this entity remains unknown. Multifocal choroiditis is an uncommon, chronic, recurrent disease, which affects females more than males by a ratio of 3:1 or greater and usually presents with varying degrees of visual loss depending on the lesion locations. The choroidal lesions are numerous, are often yellow or yellowish grey and round or oval in nature and are seen at the level of the RPE or choriocapillaris. Most lesions are small, 50–100 μm, but can also be larger and can be associated with varying amounts of sub-retinal fluid. As the lesions resolve, they become atrophic and can appear punched out with varying degrees of pigment and scarring around the outside or within the lesion. Lesions are more commonly seen in the peripapillary region, in the posterior pole or in the midperiphery and may be arranged singly, in clusters or in linear or concentric streaks known as Schlagel lines.

MFC may be complicated, not uncommonly, by inflammatory CNV (Cunningham et al., 2016). Visual prognosis in MFC may be limited by disruption of the retina and RPE due to inflammation and/or CNV (Vance et al., 2011). Making the distinction between inflammatory lesions versus iCNV is mandatory to optimize therapy. Treatment of inflammatory lesions relies on local and/or systemic steroids and immunosuppressant therapy (D'Ambrosio et al., 2014), while the common practice for the management of iCNV relies on the administration of intravitreal anti-vascular endothelial growth factor (anti-VEGF) agents. Even with advanced multimodal imaging, the differentiation between active inflammatory infiltrates and iCNV may be challenging because both lesion types have the potential to cause tissue disruption and breakdown in the blood–retina barrier (Haen and Spaide, 2008; Kotsolis et al, 2010).

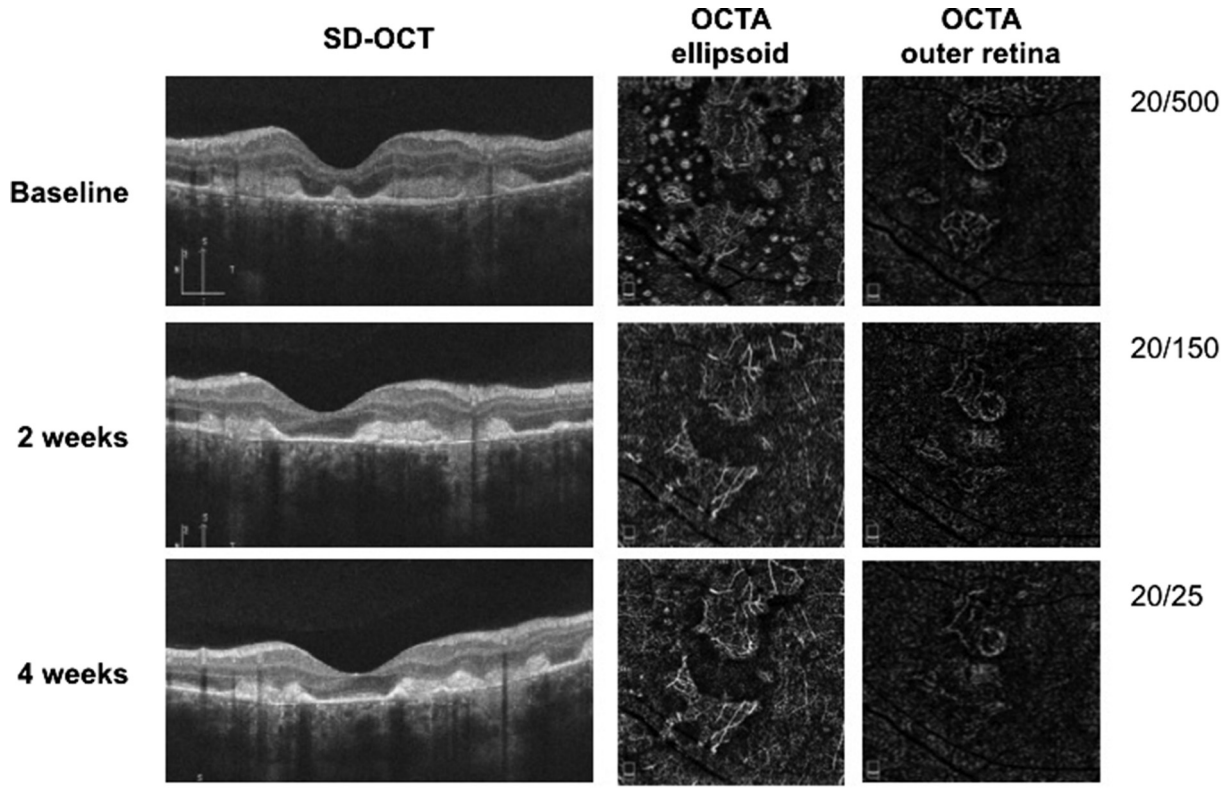

Fig. 10. *Sequential OCTA of a multifocal choroiditis patient after steroid treatment.* The figure report in the top row the baseline OCT appearance of the MFC patients from Fig. 10. Baseline OCT showed smaller conical lesions located above the RPE, and broader hyperreflective lesions with rupture of the above RPE. OCTA at the level of the ellipsoid mirrored these 2 different kind of lesions, but only the larger ones have an actual vascular net inside, as highlighted with an OCTA of the outer retina, normally avascular. The patient was treated with oral prednisone 60 MG. At the 2 week follow up visit (middle row), the patient's vision in the left eye improved to 20/150, and on SD-OCT the inflammatory conical lesions resolved with no visible alteration, while the broader RPE elevations consistent with iCNV decreased in thickness. Sequential OCTA illustrated disappearance of the smaller lesions on the ellipsoid zone, confirming their inflammatory nature, and progressive resolution of the larger neovascular lesions in the outer retina. At the 4 weeks follow up (bottom row), visual acuity had improved to 20/25, and on OCTA the lacy vascular nets in the outer retina had further reduced but not resolved, suggesting the need for anti-vascular endothelial growth factor intravitreal injection.

Fig. 9 illustrates different scans on OCTA and SD-OCT (panels C and D) of the left eye of a 27-year-old white woman with newly diagnosed MFC. On SD-OCT two different patterns of RPE detachment associated with homogeneous internal material of medium reflectivity were identified. The first were small conical RPE detachments while the second were broader in horizontal diameter but similar in height, and illustrated RPE dehiscence associated with diffusion of infiltrate into the outer retina. 3 × 3-mm OCTA with segmentation at the RPE failed to detect blood flow inside these smaller lesions with the intact RPE. The larger lesions with RPE dehiscence however, demonstrated associated neovascularization (Fig. 10).

Cheng et al. (2016) investigated 52 eyes with MFC and active lesions using multimodal imaging and OCTA. In their study, the authors detected 23 inflammatory choroidal neovascular membranes that on FA exhibited the classic appearance, with early well defined hyperfluorescence and late leakage. Of these 23 neovascular lesions, OCTA demonstrated well-circumscribed vascular networks of different shapes in 20 cases. Three (13%) of these lesions were purely type I on SD-OCT with an intact overlying RPE and illustrated vascular flow with OCTA. At the same time, the authors identified 32 lesions that showed no blood flow signal by OCTA and were therefore classified as purely inflammatory. On FA, these lesions demonstrated various patterns including hypofluorescence (41.2%), isofluorescence (35.3%) and hyperfluorescence (23.5%), in the early phase, and all showed leakage in the late phase. On SD-OCT, these lesions presented as sub-RPE hyperreflective homogeneous material in 12/32 cases (35.3%).

Recently, Zahid et al. (2016) retrospectively analyzed the OCTA findings in 18 eyes with MFC. Only 2 of their eyes demonstrated purely sub-RPE lesions with no evidence of neovascular flow on OCTA. Eleven eyes in their series illustrated purely sub-retinal lesions that demonstrated neovascular flow on OCTA. Five eyes had mixed sub-RPE and subretinal lesions and OCTA flow was detected in all 5 cases, either active (1/5 eyes) or inactive (4/5 eyes). Their use of OCTA to detect the neovascular nature of the MFC lesions resulted in a much higher frequency (83%) of neovascularization in MFC than previously reported in the literature with conventional dye-based imaging (23% in 122 eyes reported by Thorne et al., (2006)). Once again, OCTA demonstrated a higher sensitivity in detecting neovascular flow within MFC lesions but a lower specificity in determining which lesions were clinically active.

More importantly, the absence of neovascular flow by OCTA in sub-RPE lesions in Zahid's 2 patients and in our isolated case report may offer insight into the pathophysiology of MFC. This observation suggests that the progression of neovascularization in MFC may be intrinsically linked to the integrity of the RPE. The rare histopathologic studies of MFC lesions illustrate the presence of choroidal infiltrates comprised of B-cell lymphocytes (Shimada et al., 2008). The inflammatory cytokines thus produced lead to breakdown of Bruch's membrane and solid RPE avascular detachments. Progressive inflammatory breakdown of the RPE may result in an egress of infiltrate into the outer retina and may provide a conduit for pathological angiogenesis.

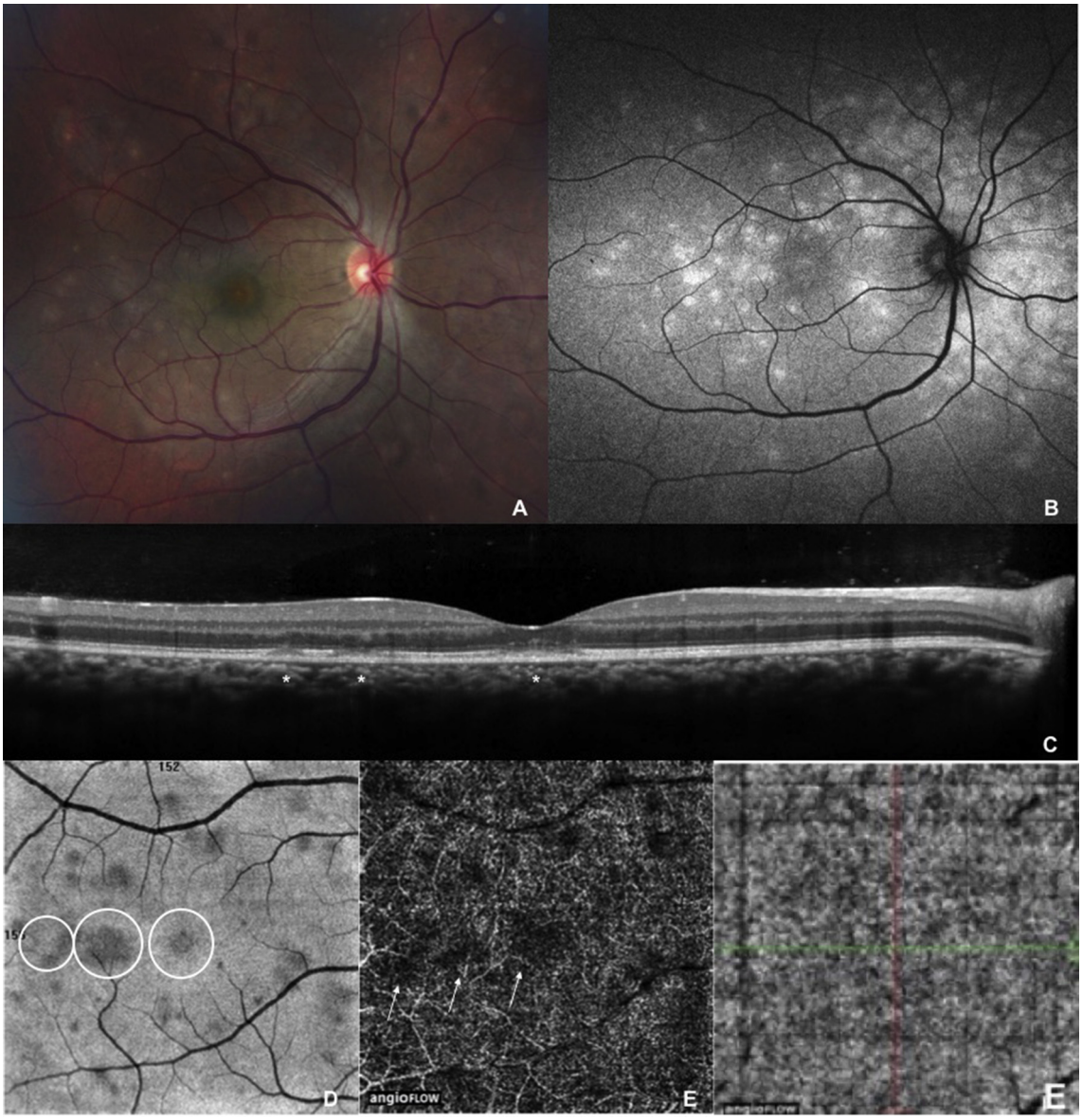

Fig. 11. *Multimodal imaging of a patient with multiple evanescent white dot syndrome.* Color fundus photography of a 22-year-old female patient with MEWDS (A) highlights classic large white lesions that on fundus autofluorescence (B) appear hyperautofluorescent. An OCT scan through the MEWDS lesion (C) detects mottling of the RPE (responsible for the increased autofluorescence) and attenuation of the ellipsoid (asterisks). An en face slab at the level of the ellipsoid (D) illustrate hyporeflective spots (white circles) that corresponds to the creamy fundus lesions and to the RPE hypertrophy (D). Optical coherence tomography angiography of the superficial (E) capillary plexus shows "projection artifacts": the MEWDS lesions seem to have no flow (arrows), whereas these are just the results of the underlying RPE mottling. An OCTA at the level of the choriocapillaris (F) failed to demonstrate any evidence of flow void or flow disturbance, thus disproving previous theories that MEWDS lesions are localized in the choriocapillaris.

On the other hand, Levison et al. (2016b) in their series of 5 MFC patients noted that in eyes with hyper-reflective material entirely under the RPE, OCTA tended to reveal mature vascular formations consistent with CNV.

Although certain authors (Zahid et al., 2016) have proposed that the status of the RPE above a MFC lesion may predict the presence or absence of flow in the lesion, it seems more plausible that RPE disruption is the result, and not the cause, of inflammatory CNV as noted by Cheng et al. (2016). While in older patients with age-related macular degeneration the RPE/Bruch complex is less adherent and neovascularization more typically grows under the RPE (type 1 neovascularization [Grossniklaus and Gass, 1998]), in young MFC patients active neovascular lesions more commonly erode and break through the RPE and grow in the subretinal space (type 2 neovascularization). In patients with MFC, type 1 neovascularization may be latent, inactive and difficult to identify with OCTA; when active, these lesions are more likely to break through the RPE and be detected in the subretinal space as type 2 neovascularization.

FA is currently the gold standard for identifying CNV (Cheng et al., 2016). The typical presentation of CNV on FA is early hyperfluorescence with late leakage, while inflammatory infiltrates illustrate early hypofluorescence or isofluorescence with late hyperfluoresence. Although the different characteristics on FA may be used to differentiate these 2 kinds of lesions, there are exceptions to the rule. For example, CNV may fail to demonstrate obvious early hyperfluorescence due to blockage from the inflammatory component, fluid or hemorrhage (Spaide et al., 2015b). Further inflammation may be hyperfluorescent in the early stage because of RPE damage causing a window defect. It is therefore challenging to

distinguish CNV from inflammatory lesions by FA.

In MFC patients, OCTA has shown remarkable precision in distinguishing CNV (Jia et al., 2014) from inflammatory lesions that were poorly differentiated using other imaging modalities. However, OCTA has demonstrated limitations in differentiating active neovascularization versus an inactive scar (Levison et al., 2016b). FA may provide insightful information in these cases. Cheng et al. (2016) identified 3 cases of "quiescent CNV" without active leakage on FA but with OCTA a blood flow signal and detailed microvascular identification of the CNV was noted. The authors hypothesized that these cases of "quiescent CNV" consisted of mature vessels associated with fibrotic tissue. These angiogenic lesions do not require treatment but should be closely monitored as the natural history is unknown.

In summary, OCTA may provide reliable identification of CNV when dye-based angiography may be inconclusive (Levison et al., 2016a, 2016b). OCTA can aid clinicians in the recognition of inflammatory choroidal neovascular lesions and can guide follow up assessment and response to treatment. Studies are however not conclusive and more robust scientific evidence is required to validate the role of OCTA in the clinical assessment and management of MFC patients with inflammatory CNV.

7. Optical coherence tomography angiography of the choriocapillaris in uveitis

Optical coherence tomography angiography imaging of the choroid will enable the clinician to more reliably identify and monitor the course of choriocapillaris ischemia to better guide diagnosis and management and may provide a biomarker to assess the need for systemic treatment and the duration of immunosuppressant therapy.

7.1. Multiple evanescent white dot syndrome

Multiple evanescent white dot syndrome (MEWDS), first reported by Jampol et al., in 1984, is an acute-onset inflammatory syndrome characterized by multiple yellow-white dots and spots (Fig. 11, panel A), 100 to 200 μm in size, that are deep to the retina. Although the clinical features of MEWDS are well described, the etiology is still unknown. Fluorescein angiographic findings (Boretsky et al., 2013; Shahlaee et al., 2015) include speckled hyperfluorescence of the white spots in a wreath-like pattern of dots, and electroretinography analysis (Moschos et al., 2014; Yamamoto et al., 2003) demonstrates photoreceptor dysfunction with a decreased a-wave amplitude, suggesting that the location of the disease process resides in the outer retina and/or the RPE. The specific deficit was hypothesized to be due to a misalignment of photoreceptors accounting for the foveal granularity specific to this disease. Photoreceptor disruption was initially attributed to a primary RPE abnormality, since the hyper-fluorescent FA pattern in MEWDS was interpreted as an RPE window defect. With the widespread clinical use of ICGA in the 1990s, MEWDS was interpreted as a choroidopathy (Dell'omo et al., 2010). Early-phase ICGA discredited the FA-based concept of RPE window defects (Dell'omo et al., 2010). The observation of late-phase ICG hypofluorescence suggested a choroidal origin of MEWDS lesions resulting from choroidal hypoperfusion. The "choroidal" lesions were thought to perturb the RPE and outer retina sufficiently to account for the characteristic white spots. To reconcile these findings, MEWDS has been termed "a chorioretinopathy with varying degrees of choroidal and retinal involvement" (Dell'omo et al., 2010; Jampol et al., 1984; Shahlaee et al., 2015).

Recently, Pichi et al. (2016d) published a series of 36 eyes of 36 patients with unilateral MEWDS, evaluated with multimodal retinal imaging. Optical coherence tomography angiography was used to evaluate blood flow within the retinal capillary and choroidal circulations in acute MEWDS. The superficial and deep retinal capillary networks and the choroidal vasculature were entirely unremarkable (Fig. 11, panels E-F) and were comparable to normal capillary networks reported in healthy, control eyes. Optical coherence tomography angiography illustrated completely normal choriocapillaris flow with no evidence of vessel dilation or flow deficit even in the corresponding areas of ICG hypofluorescence. In the Pichi series (2016), the hypofluorescent "spots" identified with ICGA precisely co-localized with areas of inner segment ellipsoid loss very well defined with "en-face" OCT (Fig. 11, panel D). The cause of choroidal hypofluorescence was therefore difficult to explain given the normal choroidal findings with OCTA. Chang et al. (2005) studied the ICG absorption characteristics of the RPE and noted that the RPE normally absorbs ICG causing physiological background hyperfluorescence. ICG RPE uptake however may be disrupted in certain retinal disorders, such as MEWDS, and may explain the late hypofluorescent lesions that co-localize with the associated areas of ellipsoid loss, as documented in this study. Optical coherence tomography angiography of MEWDS has for the

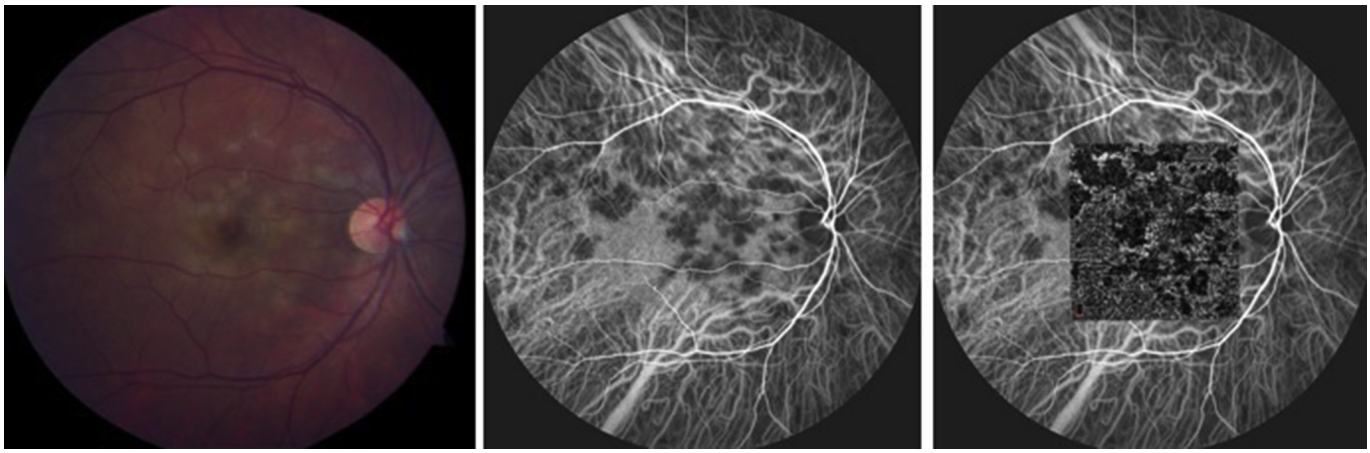

Fig. 12. *Right eye of a patient with acute posterior multifocal placoid pigment epitheliopathy.* Color fundus photograph of right eye demonstrates multifocal placoid lesions of the posterior pole at baseline (A). Corresponding mid-phase indocyanine green angiography illustrates hypofluoresence, indicative of ischemia. *En face* OCTA at the level of choriocapillaris is superimposed on ICGA and demonstrates remarkable flow voids that precisely colocalize with ICG hypofluorescent lesions. The combined use of ICGA and OCTA allows to localize the placoid lesions at the level of the choroid.

first time been paramount in supporting the hypothesis that the choriocapillaris may not be involved in this disease and that MEWDS may be primarily the result of an abnormality at the level of the RPE-photoreceptor complex.

7.2. Acute posterior multifocal placoid pigment epitheliopathy

Acute posterior multifocal placoid pigment epitheliopathy (APMPPE) was first described by Gass in 1968. Gass chose the term 'pigment epitheliopathy' to reflect the most significant clinical tissue involvement. Other groups in that era noted the presence of severely depressed electrooculogram (EOG) testing indicating dysfunction of the retinal pigment epithelium. However, controversy has persisted regarding the pathogenesis of APMPPE since its initial description. After Gass' initial report (1968), Deutman et al. (1972) proposed that the RPE abnormalities in APMPPE were due to ischemia of the choriocapillaris. More recent studies utilizing ICGA (Mrejen et al., 2016) have provided additional insights into APMPPE and have supported choroidal involvement as a prominent feature. As originally described, however, several features of APMPPE remained atypical for a choroiditis including the rapid resolution of lesions and the near absence of damage to the choroid despite significant alternations in the RPE. For this reason, a later study (Deutman et al., 1973) employing fluorescein angiography proposed acute inflammation of the choriocapillaris affecting the RPE but not the medium and large sized choroidal vessels (Spaide et al., 1991). With the advent of spectral domain optical coherence tomography (SD-OCT), several studies (Mrejen et al., 2016) have demonstrated increased inner choroidal hyporeflectivity or lucency in APMPPE that is thought to correspond to inflammation of the inner choroid or the choriocapillaris.

Klufas et al. (2017) utilized *en face* OCT and OCTA technology to investigate the level of disease in APMPPE and other placoid related disorders and to assess the choroid for decreased microvascular blood flow. They recruited a total of 25 eyes of 15 patients with a diagnosis of placoid disease from three ophthalmology clinics and dynamically examined 30-μm OCTA and en face OCT slabs from the outer retina to the outer choroid. Of the 25 eyes, 96% (N = 24/25) with placoid disease on multimodal imaging demonstrated evidence of inner choroidal or choriocapillaris flow reduction or ischemia on analysis of segmented OCTA scans that correlated with onset of visual symptoms. In all affected eyes, review of *en face* structural OCT images revealed circumscribed areas of hyporeflectivity at the level of the ellipsoid zone/RPE complex that co-localized to the area of reduced choriocapillaris flow on corresponding OCTA. The zone of choriocapillaris ischemia as visualized by OCTA was the same or greater than the area of hypofluoresence on ICGA (Fig. 12). The authors carefully assessed for signal attenuation and were able to determine that the OCTA lesions were predominantly the result of a true inner choroidal flow void (presumably ischemia) rather than shadowing from the outer retinal placoid lesions. The authors therefore concluded that ICGA hypofluorescence was indeed the result of decreased inner choroidal or choriocapillaris flow rather than blockage from overlying RPE changes. Review of those placoid cases with longitudinal follow-up illustrated resolution of the choriocapillaris ischemia and the outer retinal changes with treatment or disease course. This study by Klufas et al. (2017) indicated that OCTA may provide an important noninvasive, fast and simple biomarker of disease to guide diagnosis, prognosis and therapeutic response in patients with placoid related disorders and may help differentiate these overlapping disorders (e.g. APMPPE, Relentless Placoid Chorioretinitis and Persistent Placoid Chorioretinopathy) on the basis of inner choroidal ischemia (Dolz-Marco et al., 2017).

Salvatore et al. (2016) recently described a 27-year-old man with APMPPE and OCTA findings consistent with those reported by Klufas et al. (2017). The choriocapillaris was imaged with OCTA with segmentation below the retinal pigment epithelium and alterations in the capillary density and microvascular morphology of the inner choroid were evident. Features that the authors reported included disruption of the typical packed honeycomb structure of the inner choroid at the central fovea within placoid lesions indicating reduction of choriocapillaris flow. These OCT angiographic areas of nonperfusion corresponded to the lesions observed on FA and ICGA. Repeat OCTA images (at 3, 11, and 21 days after presentation) demonstrated recovery in choriocapillaris flow, with progressive evidence of reduction in extent of the nonperfused areas and signs of vascular reperfusion.

7.3. Multifocal choroiditis

Cerquaglia et al. (2016) described a 45-year-old man with MFC who presented with severe vision loss and a central scotoma in his left eye. Deep to Bruch's membrane, at the level of the choriocapillaris, flow signal loss was noted; this signal void area, probably due to altered blood flow or frank loss of the choriocapillaris, precisely co-localized to the hypofluorescent lesion with late phase ICGA. A hyperintense vascular network within the hypointense area at the level of the choriocapillaris was identified. This finding was attributed to Sattler's layer vessels and was noted to have a bright vascular flow signal because of the complete absence of vascular flow originating from the choriocapillaris. SD-OCT also showed RPE atrophy in the same area.

7.4. Serpiginous-like choroiditis

The serpiginous choroiditis group consists of four overlapping disorders that differ essentially in the pattern of placoid progression:

- Classic serpiginous choroiditis
- Macular serpiginous choroiditis
- Serpiginous-like choroiditis
- Ampiginous choroiditis

Typically all are rare, often bilateral, chronic, relapsing diseases associated with progressive inflammation and scarring of the retinal pigment epithelium (RPE) and inner choroid.

Serpiginous-like choroiditis differs from classic serpiginous choroiditis (Bansal et al., 2012a,b) in that the choroiditis is multifocal. Most cases of serpiginous-like choroiditis are bilateral and affect predominantly middle-aged males. Patients often have multifocal lesions that progress to confluent, diffuse choroiditis finally resembling classic serpiginous choroiditis. Others may present with a progressive plaque-like, amoeboid pattern of choroiditis similar to ampiginous choroiditis. Remarkably, the macula is spared in most patients; thus, the visual outcomes may be better than in classic serpiginous choroiditis which is associated with a poor visual prognosis. Patients with serpiginous-like choroiditis usually develop vitritis in association with active ocular lesions (Vasconcelos-Santos et al., 2010). Gupta and colleagues (Gupta et al., 2003a,b) originally reported on seven patients with positive tuberculin skin tests, constitutional symptoms, chest radiographs compatible with pulmonary tuberculosis, and choroidal inflammation similar to serpiginous choroiditis. Since the original publication, the association of serpiginous-like choroiditis with *Mycobacterium tuberculosis* has been strengthened by its PCR confirmation in the vitreous and aqueous fluid in the majority of affected eyes (Mandadi et al., 2016).

Optical coherence tomography angiography has been useful in

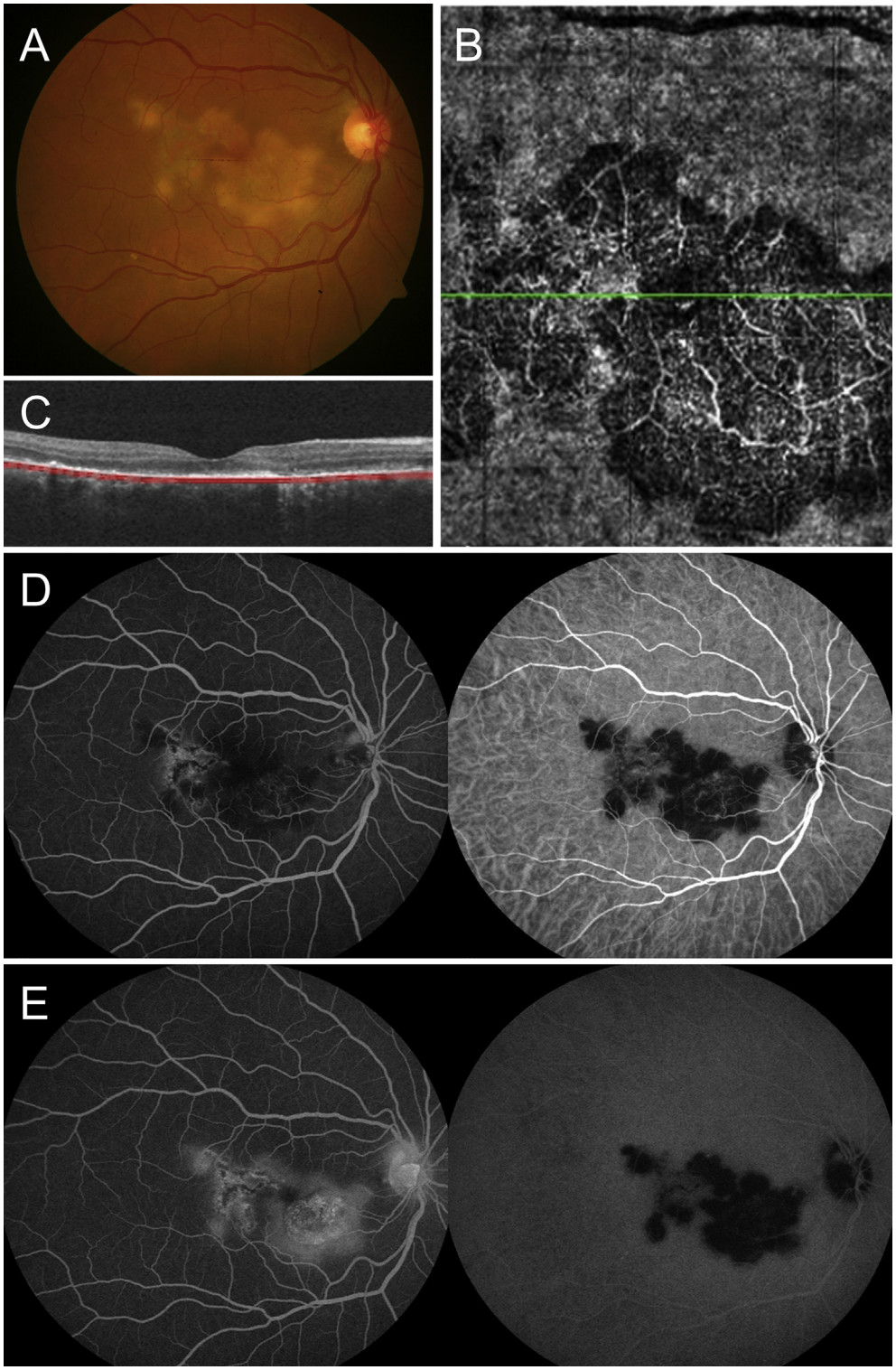

Fig. 13. *Multimodal imaging of a 45-year-old female of Asian Indian ethnicity diagnosed with tubercular serpiginous-like choroiditis.* Color fundus photograph (A) illustrates characteristic yellow-white active placoid lesions involving the central macula of the right eye. Optical coherence tomography angiography *en face* image through the central macular area demonstrates a significant flow void at the level of the inner choroid with associated projection artifact from the overlying retinal vessels (B). The corresponding OCT B-scan (C) illustrates the lesion involving the outer retina, RPE, choriocapillaris and inner choroid. Combined fluorescein angiography (FA) and indocyanine green angiography (ICGA) in the early frame (D) shows hypofluorescence in the region of the placoid choroiditis. Late frame of FA (E) illustrates late staining. Late phase of ICGA (E) demonstrates persistent hypofluorescence corresponding to the OCTA image suggestive of true choriocapillaris ischemia.

detecting choriocapillaris ischemia and atrophy as well as the development of choroidal neovascularization in these disorders and can be used as a tool to monitor these lesions.

Recently, Mandadi et al. (2016) completed a prospective study on 18 eyes of 18 patients with tubercular serpiginous-like choroiditis and selected study lesions that were located in the posterior

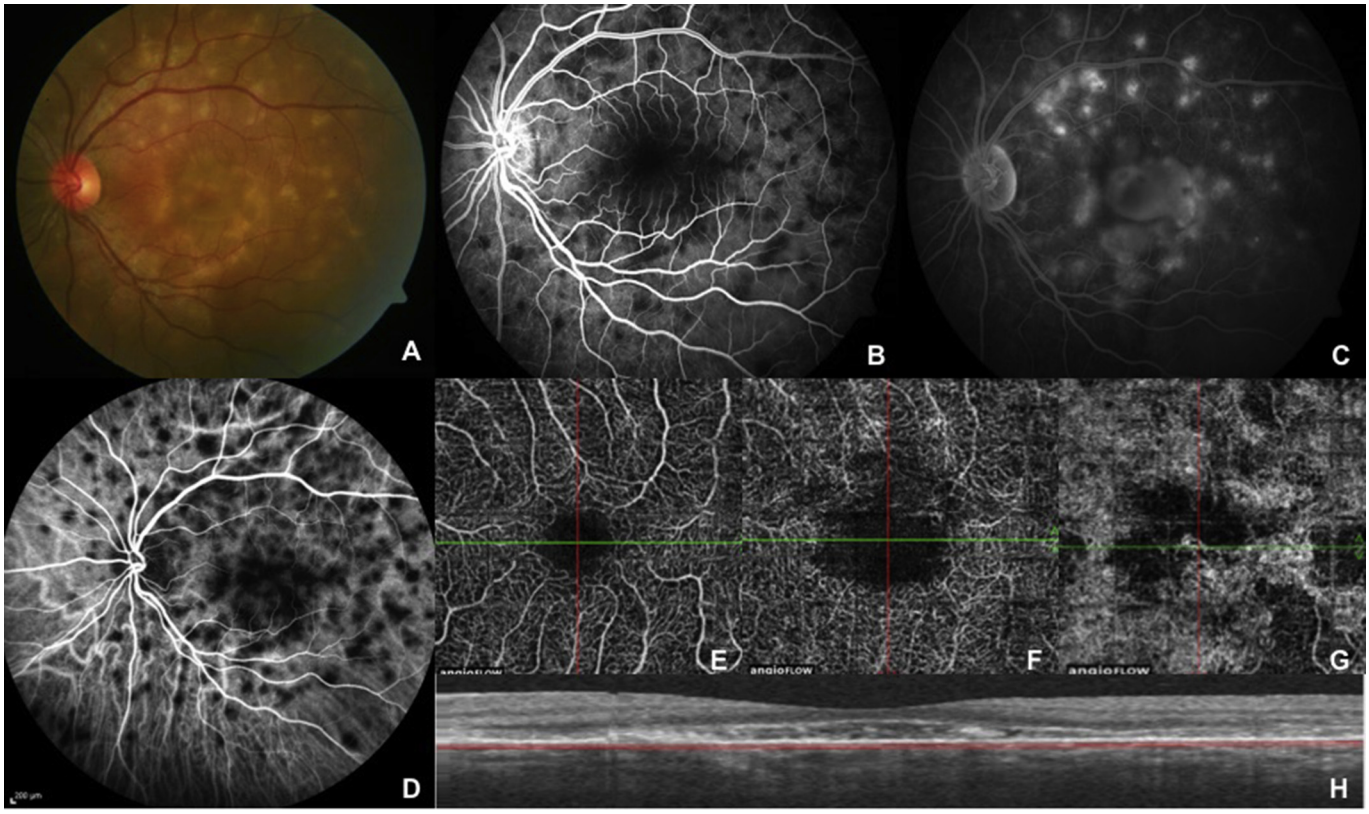

Fig. 14. *Multimodal imaging of a patient with Vogt-Koyanagi-Harada disease*. Vogt-Koyanagi-Harada is a disease of the melanocytes and as such the ocular manifestations involve primarily the choroid with subsequent involvement of the retinal pigment epithelium (RPE). In the acute stage, fundus examination reveals small nodules at the level of the RPE, known as Dalen-Fuchs nodules, in the posterior pole. Fluorescein angiography reveals early masking from the RPE nodules (B) and late multifocal areas of pinpoint leakage and pooling within subretinal fluid (C). Indocyanine green angiography (D) indicate active inflammation at the level of the choroid as dark spots. Optical coherence tomography angiography shows no changes in the superficial capillary layer (E), some rarefaction of the deep capillary layer (F), and most importantly areas of flow void at the level of the choriocapillaris (G), proving that the choriocapillaris may also be involved, especially in recurrent cases, resulting in localized ischemic abnormalities.

pole and were active. Optical coherence tomography angiography was performed using Optovue RTVue XR 100 Avanti (Optovue Inc., Fremont, CA, USA). The same lesions were also imaged with color fundus photography (Fig. 13, panel A), fundus autofluorescence, fluorescein and indocyanine green angiography (Fig. 13, panel D and E) and enhanced depth OCT imaging (Fig. 14, panel C). The OCTA images visualized on the OptoVue software were analyzed and enface OCTA maps were compared with the FA and ICGA findings. Additionally, the structural characteristics of the choroidal vasculature were compared with EDI-OCT. The superficial and deep retinal capillary plexus were normal in all eyes on OCTA. For the assessment of the choriocapillaris layer, the segmentation line was placed below the RPE-Bruch's membrane complex. All eyes demonstrated areas of reduced perfusion or 'flow void' in the areas corresponding to both active and healed choroiditis lesions with OCTA (Fig. 13, panel B). During the active stage of the disease, the OCTA areas of flow-void were clearly demarcated with ICGA and demonstrated hypofluorescence throughout the study. Point-to-point registration, between the hypofluorescent lesions illustrated on ICG and the areas of flow-void demonstrated on OCTA, was precisely noted. Additionally, intervening areas of preserved choriocapillaris and medium-sized choroidal vessels were identified between the active lesions. As the lesions healed, deeper medium-to-large choroidal vessels became more prominent and were better delineated on OCTA than on ICG. The areas of flow void on OCTA were also analyzed using EDI-OCT to characterize the anatomical correlate. In one patient, the area of flow-void was attributable to decreased signal transmission due to outer retinal layers deposits identified with EDI OCT. However, none of the other lesions demonstrated decreased signal transmission on cross-sectional or enface OCT, thus indicating the presence of true 'flow-void'. On EDI OCT, these areas of flow-void were seen as 'hyporeflective' areas of thickened choriocapillaris. However, lesions during the healing stage in which underlying medium-to-large choroidal vessels were demonstrated with OCTA, corresponded to choriocapillaris atrophy on EDI OCT. This study indicated a good morphological correlation between the OCTA, ICG and EDI OCT abnormalities.

In another study, the same group (Agarwal et al., 2016) reported the OCTA features of 5 patients with SLC who developed paradoxical worsening upon initiation of anti-tubercular therapy. OCTA demonstrated that paradoxical worsening of these lesions was associated with increase in the areas of 'flow-void' that corresponded to active choroiditis infiltrates. These lesions tended to expand and coalesce with loss of the intervening normal appearing tissue. The active edge was hyperautofluorescent and corresponded to areas of flow-void on OCTA. This study demonstrated that OCTA may provide a simple, fast, noninvasive and high-resolution imaging system to document progressive or recurrent choriocapillaris hypoperfusion essential in the monitoring and follow up of serpiginous patients and obviating the need for repeat dye based angiography.

7.5. Birdshot chorioretinopathy

de Carlo et al. (2015) performed an OCTA analysis of 8 eyes of 4 patients with BSCR and employed a 10 μm slab of the

Table 1
Different uveitis entities have different findings on the various layers of OCTA.

	INFLAMATORY VASCULITIS	BIRDSHOT CHORIORETINOPATHY	UVEITIC MACULAR EDEMA	INFLAMMATORY CNV	PIC/MFC	MEWDS	APMPPE	SERPIGINOID CHOROIDITIS	VKH
SUPERFICIAL CAPILLARY PLEXUS	- Decreased capillary density - Decreased branching	- Telangiectatic vessels - Enlarged FAZ - Decreased capillary density	- No change						
DEEP CAPILLARY PLEXUS	- Decreased capillary density (less profound than SCP)	- Decreased capillary density (more profound than SCP)	- Decreased capillary density						
OUTER RETINA				- Neovascular network	- No flow				
CHORIOCAPILLARIS		- Normal flow in active lesions - Reduced flow in atrophic healed lesions			- Focal flow reduction	- Normal flow	- Flow reduction and ischemia	- Flow reduction in areas of active choroiditis	- Focal flow void
CHOROID							- Flow reduction and ischemia	- Vessels better delineated in areas of healed choroiditis	

choriocapillaris directly below Bruch membrane to search for choroidal vascular changes. Four of the 8 eyes (50%) illustrated depigmented and atrophic birdshot lesions in the posterior pole on fundus photography that co-localized to the OCT angiographic absence of choriocapillaris flow beneath the disrupted retinal pigment epithelium. Their OCTA findings of complete loss or reduced choroidal blood flow is consistent with advanced birdshot lesions in which a chronic granulomatous reaction can ultimately destroy uveal melanocytes and cause atrophy of the inner choroidal stroma.

Pichi et al. (2016a,b,c,d) reviewed a series of 44 BSCR eyes examined with OCTA and scanned the choriocapillaris and the inner choroid, but could not detect any association between the creamy, yellow active birdshot lesions and disturbances in the choriocapillaris flow. This is due to the fact that early birdshot lesions are inflammatory choroidal infiltrates consisting of epithelioid cells surrounding choroidal stromal melanocytes. These active choroidal lesions are partial thickness and do not affect the adjacent choriocapillaris early in the course of disease explaining the normal OCTA analysis of the choroid. Once these lesions depigment, the granulomas resolve with atrophy of the choriocapillaris and inner stroma that can be detected by means of OCTA.

7.6. Vogt koyanagi harada

Vogt-Koyanagi-Harada (VKH) disease is regarded as a multisystem granulomatous disease affecting the eyes, integumentary system, meninges, and the auditory system. An association with ocular inflammation and poliosis was reported by Vogt in 1906. Harada (1926) and Koyanagi (1929) independently described ocular inflammation associated with cerebrospinal fluid pleocytosis and dermal depigmentation, respectively. Later, the disorders described by Vogt, Koyanagi, and Harada were considered to be the same disease process, which came to be known as VKH. Vogt-Koyanagi-Harada disease involves a T-lymphocyte-mediated autoimmune process directed against antigen(s) such as tyrosinase peptides associated with melanocytes.

The ophthalmic manifestations typically consist of four stages. The initial prodromal stage is remarkable for systemic features including meningeal findings. The acute ocular stage follows and is associated with exudative retinal detachment (Fig. 14, panel A). A convalescent stage, remarkable for pigment loss affecting various organ systems, may ensue. Finally the last stage is notable for chronic anterior uveitis that can last several months or even years. This staging system is considerably variable and patients may present only with findings of the acute ocular phase of VKH with classic exudative retinal detachment and signs of uveitis.

While the granulomatous lesions have been extensively studied, the available knowledge of inner choroidal vascular abnormalities in VKH is rather limited. Histopathologic studies have shown that while VKH disease primarily affects the choroidal stroma with diffuse infiltration of inflammatory cells, the choriocapillaris may also be involved, especially in recurrent cases, resulting in localized ischemic abnormalities (Rao, 2007). The inflammation primarily involves the choroidal stroma with subsequent involvement of the retinal pigment epithelium (RPE) and outer retina (Liu et al., 2016).

Aggarwal et al. (2016) prospectively examined 10 eyes of 10 VKH patients with multimodal imaging and OCTA (Optovue RTVue XR 100 Avanti® (Optovue Inc., Fremont, CA). The choroidal microvascular abnormalities on OCTA were compared with the findings identified with EDI-OCT. Choriocapillaris ischemia was defined on EDI- OCT as an increased thickness and hyporeflectivity of the choriocapillaris layer in the absence of characteristic hyperreflective white dots. Choroidal granulomas were identified on EDI-OCT as areas of increased homogeneity (with internal hyporeflectivity) within the choroid with loss of the typical vascular pattern and an associated increased signal transmission effect (unlike large choroidal vessels). On OCTA, the choriocapillaris layer (below the RPE-Bruch's membrane complex) illustrated multiple dark foci with loss of the choriocapillaris (or severe hypoperfusion) that appeared as areas of flow void. The edges of these areas were discrete and clearly demarcated. The hyporeflective areas of flow void on OCTA demonstrated corresponding choriocapillaris ischemia (Fig. 14, panel G)with thickening and hyporeflectivity with EDI-OCT in all the eyes. Choroidal granulomas were observed in the macula with EDI-OCT in three eyes. These lesions, located in the deeper layers of the choroid, were not evaluated by OCTA in the study. In comparing the OCTA with ICGA (Fig. 14, panel D), the areas of flow void on OCTA illustrated consistent colocalization with the persistent hypofluorescent spots with ICGA in all study patients.

Follow-up OCTA of patients with acute VKH demonstrated interval recovery in the choriocapillaris flow void areas in all the patients. Decrease in the size of these flow void areas could be confirmed in all but two patients upon initiation of treatment.

Optical coherence tomography angiography appeared to be an effective adjunct that may be sensitive in detecting the presence of disease activity in VKH. Choriocapillaris flow reduction (or severe hypoperfusion) with OCTA correlated well with other imaging techniques, such as EDI-OCT and ICGA in all the patients. An improvement in the flow void areas on OCTA among Agarwal's study participants correlated well with the decrease in the subfoveal choroidal thickness illustrated with EDI- OCT.

8. Future directions

Optical coherence tomography angiography is a fairly new technology that has been revolutionizing the medical retina world for the past 3 years. In its current form OCTA is not meant to replace conventional dye-based angiographies, but to integrate them in order to give new insight into macular pathologies. So far the application of OCTA to uveitis and inflammatory conditions has been limited, and the purpose of the present review is to summarize the current available notions (Table 1) in order for the ophthalmology community to start learning more regarding the morphologic appearance of the retinal and choroidal vasculature in inflammatory ocular diseases. A clear advantage of OCTA over conventional imaging is the ability of obtaining images at various depth, and this will greatly enhance our understanding of the pathophysiology of abnormal vascular changes in uveitis. Detailed analysis of the choroidal and retinal circulation using OCTA combined with FA, ICGA, autofluorescence, and OCT can shed light on the pathophysiological mechanisms responsible for manifestations of uveitis.

Case reports and case series on uveitis entities investigated *via* OCTA are becoming more and more important for establishing the characteristics of active versus inactive chorioretinal lesions on OCTA. This may allow in the future the detection of recurrence of uveitis earlier on OCTA by identifying changes such as flow increase or choriocapillaris ischemia.

In uveitis, there is a great need to identify more accurate, noninvasive and quantifiable biomarkers of inflammation especially with diseases such as retinal vasculitis and birdshot chorioretinopathy. Retinal vascular leakage is not yet quantifiable. Quantitating flow in the retinal capillary plexus and choroid may also help to identify uveitic eyes with active inflammation. The calculation of the area and density of microvascular flow, or the loss of flow, in the retinal capillary plexus (SCP, DCP) and in the choroid provides a unique capability to quantify vascular perfusion and ischemia in ocular disease. This powerful capability may be further enhanced with the development of technology that can quantitate the intensity of flow allowing advancement beyond an essential binary algorithm and powering clinicians and researchers to distinguish active versus inactive neovascularization.

Despite its many advantages, OCTA is still in its developmental phase with many shortcomings, especially in the field of ocular inflammation. Image artifacts and projections of superficial vessels onto lower vessels is a major challenge in identifying pathologic changes in posterior uveitis as involvement of choriocapillaris and choroidal stroma is an important component of these conditions. Other advancements in OCTA technology have already been developed including algorithms to remove projection artifact. Applying this novel technology to uveitis patients will improve the accuracy with which we are assessing the DCP for ischemia.

At the same time, we need to develop better methods to distinguish signal attenuation and shadowing from true flow deficits. This will markedly improve our ability to manage uveitis conditions with choroidal ischemia. The use of swept source OCTA can potentially improve our efficacy in the management of choroidal disorders due to improved signal penetration and will improve our ability to differentiate inner choroidal from outer choroidal disorders.

Despite all these advances, in its current state OCTA serves as a useful adjunct to the traditional angiographic techniques, since multimodal image analysis is still necessary to confirm pathologic findings in uveitis. However, with further technological development, it may reduce the need for traditional angiographic evaluations in the future.

Funding

This research did not receive any specific grant from funding agencies in the public, commercial, or not-for-profit sectors.

References

Agarwal, A., Aggarwal, K., Deokar, A., Mandadi, S.K., Singh, S.R., Singh, R., Sharma, A., Bansal, R., Gupta, V., OCTA Study Group, 2016. Optical coherence tomography angiography features of paradoxical worsening in tubercular multifocal serpiginoid choroiditis. Ocul. Immunol. Inflamm. (Sep 6), 1–10 [Epub ahead of print].

Aggarwal, K., Agarwal, A., Mahajan, S., Invernizzi, A., Mandadi, S.K., Singh, R., Bansal, R., Dogra, M.R., Gupta, V., OCTA Study Group, 2016. The Role of Optical Coherence Tomography Angiography in the Diagnosis and Management of Acute Vogt-Koyanagi-Harada Disease. Ocul. Immunol. Inflamm. (Jul 20), 1–12.

Antcliff, R.J., Stanford, M.R., Chauhan, D.S., 2000. Comparison between optical coherence tomography and fundus fluorescein angiography for the detection of cystoid macular edema in patients with uveitis. Ophthalmology 107, 593–599.

Bachmann, A.H., Villiger, M.L., Blatter, C., Lasser, T., Leitgeb, R.A., 2007. Resonant Doppler flow imaging and optical vivisection of retinal blood vessels. Jan 22 Opt. Express 15 (2), 408–422.

Bansal, R., Gupta, A., Gupta, V., 2012a. Imaging in the diagnosis and management of serpiginous choroiditis. Int. Ophthalmol. Clin. 52, 229–236.

Bansal, R., Gupta, A., Gupta, V., Dogra, M.R., Sharma, A., Bambery, P., 2012b. Tubercular serpiginous-like choroiditis presenting as multifocal serpiginoid choroiditis. Ophthalmology 119 (11), 2334–2342.

Bessette, A.P., Baynes, K., Lowder, C.Y., Levison, A.L., Pichi, F., Sharma, S., Kaiser, P.K., Srivastava, S.K., 2016. Qualitative and quantitative analysis of optical coherence tomography angiography in patients with retinal vasculitis. Retina [Epub ahead of print].

Boretsky, A., Mirza, S., Khan, F., Motamedi, M., van Kuijk, F.J., 2013. High-resolution multimodal imaging of multiple evanescent white dot syndrome. May-Jun Ophthalmic Surg. Lasers Imaging Retina 44 (3), 296–300.

Brancato, R., Bandello, F., Lattanzio, R., 1997. Iris fluorescein angiography in clinical practice. Jul-Aug Surv. Ophthalmol. 42 (1), 41–70.

Bringmann, A., Reichenbach, A., Wiedemann, P., 2004. Pathomechanisms of cystoid macular edema. Ophthalmic Res. 36, 241–249.

Cao, J.H., Silpa-Archa, S., Freitas-Neto, C.A., Foster, C.S., 2016. BIrdshot chorioretinitis lesions on indocyanine green angiography as an indicator of disease activity. Sep Retina 36 (9), 1751–1757.

Cerquaglia, A., Lupidi, M., Fiore, T., Iaccheri, B., Perri, P., Cagini, C., 2016. Deep inside multifocal choroiditis: an optical coherence tomography angiography approach. Sep Int. Ophthalmol. 2 [Epub ahead of print].

Chang, A.A., Zhu, M., Billson, F., 2005. The interaction of indocyanine green with human retinal pigment epithelium. Apr Invest. Ophthalmol. Vis. Sci 46 (4), 1463–1467.

Chen, L., Xu, G., 2013. Extensive choroidal infiltrates in choroidal biopsy proven ocular sarcoidosis. Retin Cases Brief. Rep. Winter 7 (1), 69–70.

Cheng, L., Chen, X., Weng, S., Mao, L., Gong, Y., Yu, S., Xu, X., 2016. Spectral-domain optical coherence tomography angiography findings in multifocal choroiditis with active lesions. Sep Am. J. Ophthalmol. 169, 145–161.

Choi, W.J., Pepple, K.L., Zhi, Z., 2015. Optical coherence tomography based microangiography for quantitative monitoring of structural and vascular changes in a rat model of acute uveitis in vivo: a prelimary study. J. Biomed. Opt. 20 (1).

Cunha-Vaz, J., 1979. The blood-ocular barriers. Surv. Ophthalmol. 23, 279–296.

Cunningham Jr., E.T., Ferrara, D., Mrejen, S., Freund, K.B., Zierhut, M., 2016. Imaging the choroid and choroidal neovascularization in eyes with inflammation. Jun Ocul. Immunol. Inflamm. 24 (3), 243–245.

D'Ambrosio, E., Tortorella, P., Iannetti, L., 2014. Management of uveitis-related choroidal neovascularization: from the pathogenesis to the therapy. J. Ophthalmol. 450428.

Danzig, C.J., Shields, C.L., Mashayekhi, A., Ehya, H., Manquez, M.E., Shields, J.A., 2008. Fluorescein angiography of iris juvenile xanthogranuloma. Mar-Apr J. Pediatr. Ophthalmol. Strabismus 45 (2), 110–112.

de Carlo, T.E., Bonini Filho, M.A., Adhi, M., Duker, J.S., 2015. Retinal and choroidal vasculature in birdshot chorioretinopathy analyzed using spectral domain optical coherence tomography angiography. Nov Retina 35 (11), 2392–2399.

Dehio, C., 2003. Recent progress in understanding *Bartonella*-induced vascular proliferation. Curr. Opin. Microbiol. 79 (6), 61–65.

Dell'omo, R., Wong, R., Marino, M., Konstantopoulou, K., Pavesio, C., 2010. Relationship between different fluorescein and indocyanine green angiography

features in multiple evanescent white dot syndrome. Jan Br. J. Ophthalmol. 94 (1), 59–63.
Deutman, A.F., Boen-Tan, T.N., Oosterhuis, J.A., 1973. Proceedings: acute posterior multifocal placoid pigment epitheliopathy. Ophthalmologicalogy 167 (5), 368–372.
Deutman, A.F., Oosterhuis, J.A., Boen-Tan, T.N., Aan de Kerk, A.L., 1972. Acute posterior multifocal placoid pigment epitheliopathy. Pigment epitheliopathy of choriocapillaritis? Br. J. Ophthalmol. 56 (12), 863–874.
Dolz-Marco, R., Sarraf, D., Giovinazzo, V., Freund, K.B., 2017. Optical coherence tomography angiography shows inner choroidal ischemia in acute posterior multifocal placoid pigment epitheliopathy. Retin Cases Brief. Rep. Winter 11 (Suppl. 1), S136–S143.
Dreyer, R.F., Gass, D.J., 1984. Multifocal choroiditis and panuveitis. A syndrome that mimics ocular histoplasmosis. Arch. Ophthalmol. 102, 1776–1784.
Dunn, J.P., 2015. Uveitis. Sep Prim. Care 42 (3), 305–323.
El-Asrar, A.M., Herbort, C.P., Tabbara, K.F., 2010. A clinical approach to the diagnosis of retinal vasculitis. Int. Ophthalmol. 30, 149–173.
Espinosa-Heidmann, D., Suner, I.J., Hernandez, E.P., 2003. Macrophage depletion diminishes lesion size and severity in experimental choroidal neovascularization. Invest. Ophthalmol. Vis. Sci. 44, 3586–3592.
Fingler, J., Readhead, C., Schwartz, D.M., Fraser, S.E., 2008. Phase-contrast OCT imaging of transverse flows in the mouse retina and choroid. Nov Invest. Ophthalmol. Vis. Sci. 49 (11), 5055–5059.
Fingler, J., Schwartz, D., Yang, C., Fraser, S.E., 2007. Mobility and transverse flow visualization using phase variance contrast with spectral domain optical coherence tomography. Opt. Express 15, 12636–12653.
Forrester, J.V., Liversidge, J., Dua, H.S., 1990. Comparison of clinical experimental uveitis. Curr. Eye Res. 9, 75–84.
Gass, J.D., 1968. Acute posterior multifocal placoid pigment epitheliopathy. Arch. Ophthalmol. 80 (2), 177–185.
Gass, J.D., Olson, C.L., 1976. Sarcoidosis with optic nerve and retinal involvement. Arch. Ophthalmol. 94, 945–950.
Gerstenblith, A.T., 2007. Punctate inner choroidopathy: a survey analysis of 77 persons. Ophthalmology 114 (6), 1201–1204.
Gorczynska, I., Migacz, J.V., Zawadzki, R.J., Capps, A.G., Werner, J.S., 2016. Comparison of amplitude-decorrelation, speckle-variance and phase-variance OCT angiography methods for imaging the human retina and choroid. Feb 19 Biomed. Opt. Express 7 (3), 911–942.
Grossniklaus, H.E., Gass, J.D., 1998. Clinicopathologic correlations of surgically excised type 1 and type 2 submacular choroidal neovascular membranes. Jul Am. J. Ophthalmol. 126 (1), 59–69.
Guex-Crosier, Y., 1999. The pathogenesis and clinical presentation of macular edema in inflammatory dis- eases. Doc. Ophthalmol. 97, 297–309.
Gupta, V., Gupta, A., Arora, S., Bambery, P., Dogra, M.R., Agarwal, A., 2003a. Presumed tubercular serpiginous- like choroiditis: clinical presentations and management. Ophthalmology 110, 1744–1749.
Gupta, V., Gupta, A., Arora, S., Bambery, P., Dogra, M.R., Agarwal, A., 2003b. Presumed tubercular serpiginouslike choroiditis: clinical presentations and management. Ophthalmology 110 (9), 1744–1749.
Haen, S.P., Spaide, R.F., 2008. Fundus autofluorescence in multifocal choroiditis and panuveitis. May Am. J. Ophthalmol. 145 (5), 847–853.
Harada, E., 1926. Beitrag zur klinishcen Kenntnis von nichteitriger Choroiditis (Choroiditis diffusa acuta). Acta Soc. Ophthalmol. Jpn. 30, 356–378.
Hartig, S.M., 2013. Basic image analysis and manipulation in ImageJ. Curr. Protoc. Mol. Biol. Chapter 14:Unit14.15.
Hope-Ross, M., Yannuzzi, L.A., Gragoudas, E.S., Guyer, D.R., Slakter, J.S., Sorenson, J.A., Krupsky, S., Orlock, D.A., Puliafito, C.A., 1994. Adverse reactions due to indocyanine green. Mar Ophthalmology 101 (3), 529–533.
Invernizzi, A., Mapelli, C., Viola, F., Cigada, M., Cimino, L., Ratiglia, R., Staurenghi, G., Gupta, A., 2015. Choroidal granulomas visualized by enhanced depth imaging optical coherence tomography. Mar Retina 35 (3), 525–531.
Jabs, D.A., Nussenblatt, R.B., Rosenbaum, J.T., Standardization of Uveitis Nomenclature (SUN) Working Group, 2005. Standardization of uveitis nomenclature for reporting clinical data: results of the first international workshop. Am. J. Ophthalmol. 140 (3), 509–516.
Jack, L.S., Agarwal, A., Sepah, Y.J., Nguyen, Q.D., 2016. Spatial agreement between Goldmann visual field defects and fundus autofluorescence in patients with birdshot chorioretinopathy, 2016 Dec J. Ophthalmic Inflamm. Infect. 6 (1), 18.
Jampol, L.M., Sieving, P.A., Pugh, D., Fishman, G.A., Gilbert, H., 1984. Multiple evanescent white dot syndrome. I. Clinical findings. May Arch. Ophthalmol. 102 (5), 671–674.
Jia, Y., Bailey, S.T., Wilson, D.J., 2014. Quantitative optical coherence tomography angiography of choroidal neovascularization in age-related macular degeneration. Ophthalmology 121 (7), 1435–1444.
Jia, Y., Tan, O., Tokayer, J., Potsaid, B., Wang, Y., Liu, J.J., Kraus, M.F., Subhash, H., Fujimoto, J.G., Hornegger, J., Huang, D., 2012. Split-spectrum amplitude-decorrelation angiography with optical coherence tomography. Feb 13 Opt. Express 20 (4), 4710–4725.
Kang, S., Kim, U.S., 2014. Using ImageJ to evaluate optic disc pallor in traumatic optic neuropathy. Apr Korean J. Ophthalmol. 28 (2), 164–169.
Kim, A.Y., Rodger, D.C., Shahidzadeh, A., Chu, Z., Koulisis, N., Burkemper, B., Jiang, X., Pepple, K.L., Wang, R.K., Puliafito, C.A., Rao, N.A., Kashani, A.H., 2016. Quantifying retinal microvascular changes in uveitis using spectral domain optical coherence tomography angiography (SD-OCTA). Sep. 1 Am. J. Ophthalmol. [Epub ahead of print].
Klufas, M., Phasukkijwatana, N., Iafe, N.A., Prasad, P.S., Agarwal, A., Gupta, V., Ansari, W., Pichi, F., Srivastava, S.K., Freund, K.B., Sadda, S.R., Sarraf, D., 2017. Optical coherence tomography angiography reveals choriocapillaris flow reduction in placoid chorioretinitis. Jan Ophthalmol. Retina 1, 77–91.
Kostianovsky, M., Greco, M.A., 1994. Angiogenic process in bacillary angiomatosis. Ultrastruct. Pathol. 18, 349–355.
Kotsolis, A.I., Killian, F.A., Ladas, I.D., Yannuzzi, L.A., 2010. Fluorescein angiography and optical coherence tomography concordance for choroidal neovascularisation in multifocal choroidtis. Nov Br. J. Ophthalmol. 94 (11), 1506–1508.
Koyanagi, Y., 1929. Dysakusis alopecia und Poliosis bei schwerer Uveitis nicht traumatischen Ursprungs. Klin. Monatsbl Augenheilkd 67, 194–211.
Kuehlewein, L., Bansal, M., Lenis, T.L., Iafe, N.A., Sadda, S.R., Bonini Filho, M.A., De Carlo, T.E., Waheed, N.K., Duker, J.S., Sarraf, D., 2015. Optical coherence tomography angiography of type 1 neovascularization in age-related macular degeneration. Oct Am. J. Ophthalmol. 160 (4), 739–748. e2.
Lardenoye, C.W.T.A., van Kooij, B., Rothova, A., 2006. Impact of macular edema on visual acuity in uveitis. Ophthalmology 113, 1446–1449.
Lax, A.J., Thomas, W., 2002. How bacteria could cause cancer: one step at a time. Trends Microbiol. 10, 293–299.
Leder, H.A., Campbell, J.P., Sepah, Y.J., 2013. Ultra-wide-field retinal imaging in the management of non-infectious retinal vasculitis. J. Ophthalmic Inflamm. Infect. 3 (1), 30.
Lee, J., Rosen, R., 2016. Optical coherence tomography angiography in diabetes. Dec Curr. Diab Rep. 16 (12), 123.
Leitgeb, R.A., Schmetterer, L., Hitzenberger, C.K., 2004. Real-time measurement of in vitro flow by Fourier-domain color Doppler optical coherence tomography. Opt. Lett. 29, 171–173.
Levinson, R.D., Brezin, A., Rothova, A., Accorinti, M., Holland, G.N., 2006. Research criteria for the diagnosis of birdshot chorioretinopathy: results of an international consensus conference. Jan Am. J. Ophthalmol. 141 (1), 185–187.
Levison, A.L., Baynes, K.M., Lowder, C.Y., Kaiser, P.K., Srivastava, S.K., 2016a. OCT angiography identification of choroidal neovascularization secondary to acute zonal occult outer retinopathy. Jan Ophthalmic Surg. Lasers Imaging Retina 47 (1), 73–75.
Levison, A.L., Baynes, K.M., Lowder, C.Y., Kaiser, P.K., Srivastava, S.K., 2016b. Choroidal neovascularisation on optical coherence tomography angiography in punctate inner choroidopathy and multifocal choroiditis. Br. J. Ophthalmol. Aug 18. pii: bjophthalmol-2016–308806.
Liu, X.Y., Peng, X.Y., Wang, S., You, Q.S., Li, Y.B., Xiao, Y.Y., Jonas, J.B., 2016 Nov. Features of optical coherence tomography for the diagnosis of vogt-koyanagi-harada disease. Retina 36 (11), 2116–2123.
Lynch, J.P., Kazerooni 3rd, E.A., Gay, S.E., 1997. Pulmonary sarcoidosis. Clin. Chest Med. 18, 755–785.
Maenz, M., Schlüter, D., Liesenfeld, O., Schares, G., Gross, U., Pleyer, U., 2014. Ocular toxoplasmosis past, present and new aspects of an old disease. Mar Prog. Retin Eye Res. 39, 77–106.
Mandadi, S.K.R., Agarwal, A., Agarwal, K., OCTA Study Group, 2016. Novel findings on optical coherence tomography angiography in patients with tubercular serpiginous-like choroiditis. Retina [Epub ahead of print].
Markomichelakis, N.N., Halkiadakis, I., Pantelia, E., 2004. Patterns of macular edema in patients with uveitis. Ophthalmology 111, 946–953.
Martínez-Pulgarín, D.F., Muñoz-Urbano, M., Gomez-Suta, L.D., Delgado, O.M., Rodriguez-Morales, A.J., 2015. Ocular toxocariasis: new diagnostic and therapeutic perspectives. Recent Pat. Antiinfect Drug Discov. 10 (1), 35–41.
Mason III, J.O., 2004. Retinal and optic nerve neovascularization associated with cat scratch neuroretinitis. Retina 24, 176–178.
Mehta, H., Sim, D.A., Keane, P.A., Zarranz-Ventura, J., Gallagher, K., Egan, C.A., Westcott, M., Lee, R.W., Tufail, A., Pavesio, C.E., 2015. Structural changes of the choroid in sarcoid- and tuberculosis-related granulomatous uveitis. Aug Eye (Lond) 29 (8), 1060–1068.
Michel, S.S., Ekong, A., Baltatzis, S., Foster, C.S., 2002. Multifocal choroiditis and panuveitis: immunomodu- latory therapy. Ophthalmology 109, 378–383.
Minos, E., Barry, R.J., Southworth, S., Folkard, A., Murray, P.I., Duker, J.S., Keane, P.A., Denniston, A.K., 2016. Birdshot chorioretinopathy: current knowledge and new concepts in pathophysiology, diagnosis, monitoring and treatment. May 12 Orphanet J. Rare Dis. 11 (1), 61.
Moschos, M.M., Gouliopoulos, N.S., Kalogeropoulos, C., 2014. Electrophysiological examination in uveitis: a review of the literature. Clin. Ophthalmol. 8, 199–214.
Mrejen, S., Sarraf, D., Chexal, S., Wald, K., Freund, K.B., 2016. Choroidal involvement in acute posterior multifocal placoid pigment epitheliopathy. Ophthalmic Surg. Lasers Imaging Retina 47 (1), 20–26.
Nemiroff, J., Kuehlewein, L., Rahimy, E., Tsui, I., Doshi, R., Gaudric, A., Gorin, M.B., Sadda, S., Sarraf, D., 2016. Assessing deep retinal capillary ischemia in paracentral acute middle maculopathy by optical coherence tomography angiography. Feb Am. J. Ophthalmol. 162, 121–132. e1.
Onal, S., Tugal-Tutkun, I., Neri, P., P Herbort, C., 2014. Optical coherence tomography imaging in uveitis. Apr Int. Ophthalmol. 34 (2), 401–435.
Papavasileiou, E., Miller, J.B., Sobrin, L., 2016. Swept-source optical coherence tomography findings in convalescent phase of treated sarcoid choroidal granulomas. Retin Cases Brief. Rep. Winter 10 (1), 32–36.
Park, J.J., Soetikno, B.T., Fawzi, A.A., 2016. Characterization of the middle capillary plexus using optical coherence tomography angiography in healthy and diabetic eyes. Nov Retina 36 (11), 2039–2050.
Parvan, P.R., Margo, C.E., 1996. Submacular neovascular membrane and focal

granulomatous inflammation. Ophthalmology 103, 586–589.
Peizeng, Y., Qianli, M., Xiangkun, H., Hongyan, Z., Li, W., Kijlstra, A., 2009. Longitudinal study of anterior segment inflammation by ultrasound biomicroscopy in patients with acute anterior uveitis. Mar Acta Ophthalmol. 87 (2), 211–215.
Phasukkijwatana, N., Iafe, N., Sarraf, D., 2016. Optical coherence tomography angiography of a29 birdshot chorioretinopathy complicated by retinal neovascularization. Sep Retin Cases Brief. Rep. 14 [Epub ahead of print].
Pichi, F., Baynes, K., Flachbart, C., et al., 2016a. An optical coherence tomography angiography study of the iris in anterior uveitis. ARVO e abstract 4624.
Pichi, F., Lowder, C.Y., Carrai, P., Baynes, K., Traut, C.N., Srivastava, S.K., 2016b. Macular Ischemia in Inactive Birdshot Chorioretinopathy Evaluated by OCT Angiography. AAO 2016 e poster 436.
Pichi, F., Srivastava, S.K., Levinson, A., Baynes, K.M., Traut, C., Lowder, C.Y., 2016c. A focal chorioretinal Bartonella lesion analyzed by optical coherence tomography angiography. Jun 1 Ophthalmic Surg. Lasers Imaging Retina 47 (6), 585–588.
Pichi, F., Srvivastava, S.K., Chexal, S., Lembo, A., Lima, L.H., Neri, P., Saitta, A., Chhablani, J., Albini, T.A., Nucci, P., Freund, K.B., Chung, H., Lowder, C.Y., Sarraf, D., 2016d. En face optical coherence tomography and optical coherence tomography angiography of multiple evanescent white dot syndrome: new Insights into Pathogenesis. Aug Retina 22 [Epub ahead of print].
Rao, N.A., 2007. Pathology of vogt-koyanagi-harada disease. Int. Ophthalmol. 27, 81–85.
Raviola, G., 1977. The structural basis of the blood- ocular barriers. Exp. Eye Res. 25 (Suppl. l), 27–63.
Rotsos, T.G., Moschos, M.M., 2008. Cystoid macular edema. Clin. Ophthalmol. 2, 919–930.
Salvatore, S., Steeples, L.R., Ross, A.H., Bailey, C., Lee, R.W., Carreño, E., 2016. Multimodal imaging in acute posterior multifocal placoid pigment epitheliopathy demonstrating obstruction of the choriocapillaris. Jul 1 Ophthalmic Surg. Lasers Imaging Retina 47 (7), 677–681.
Seubert, A., Schulein, R., Dehio, C., 2002. Bacterial persistence within erythrocytes: a unique pathogenic strategy of Bartonella spp. Int. J. Med. Microbiol. 291, 555–560.
Shah, R.S., Soetokno, B.T., Laijko, M., Fawzi, A.A., 2015. A mouse model for laser-induced choroidal neovascularization. Dec J. Vis. Exp. 27 (106), e53502.
Shahlaee, A., Hong, B., Sridhar, J., Mehta, S., 2015. Multimodal imaging in multiple evanescent white dot syndrome. Sep Ophthalmology 122 (9), 1836.
Shimada, H., Yuzawa, M., Hirose, T., Nakashizuka, H., Hattori, T., Kazato, Y., 2008. Pathological findings of multifocal choroiditis with panuveitis and punctate inner choroidopathy. Jul-Aug Jpn. J. Ophthalmol. 52 (4), 282–288.
Silpa-Archa, S., Maleki, A., Roohipoor, R., Preble, J.M., Foster, C.S., 2016. Analysis of three-dimensional choroidal volume with enhanced depth imaging findings in patients with birdshot retinochoroidopathy. Sep Retina 36 (9), 1758–1766.
Sivaprasad, S., Ikeji, F., Xing, W., Lightman, S., 2007. Tomographic assessment of therapeutic response to uveitic macular oedema. Clin. Exp. Ophthalmol. 35, 719–723.
Spagnolo, P., 2015. Sarcoidosis: a critical review of history and milestones. Aug Clin. Rev. Allergy Immunol. 49 (1), 1–5.
Spaide, R.F., Fujimoto, J.G., Waheed, N.K., 2015a. Image artifacts in optical coherence tomography angiography. Nov Retina 35 (11), 2163–2180.
Spaide, R.F., Klancnik Jr., J.M., Cooney, M.J., 2015b. Retinal vascular layers imaged by fluorescein angiography and optical coherence tomography angiography. JAMA Ophthalmol. 133 (1), 45–50.
Spaide, R.F., Yannuzzi, L.A., Slakter, J., 1991. Choroidal vasculitis in acute posterior multifocal placoid pigment epitheliopathy. Br. J. Ophthalmol. 75 (11), 685–687.
Symes, R., Young, M., Forooghian, F., 2015. Quantitative assessment of retinal degeneration in birdshot chorioretinopathy Using optical coherence tomography. Nov-Dec Ophthalmic Surg. Lasers Imaging Retina 46 (10), 1009–1012.
Thorne, J.E., Wittenberg, S., Jabs, D.A., 2006. Multifocal choroiditis with panuveitis incidence of ocular complications and of loss of visual acuity. Ophthalmology 113, 2310–2316.
Touhami, S., Fardeau, C., Vanier, A., Zambrowski, O., Steinborn, R., Simon, C., Tezenas du Montcel, S., Bodaghi, B., Lehoang, P., 2016. Birdshot retinochoroidopathy: prognostic factors of long-term visual outcome. Aug 11 Am. J. Ophthalmol. Ahead of print.
Tran, T.H., de Smet, M.D., Bodaghi, B., 2008. Uveitic macular oedema: correlation between optical coherence tomography patterns with visual acuity and fluorescein angiography. Br. J. Ophthalmol. 92, 922–927.
Vance, S.K., Khan, S., Klancnik, J.M., Freund, K.B., 2011. Characteristic spectral-domain optical coherence tomography findings of multifocal choroiditis. Apr Retina 31 (4), 717–723.
Vasconcelos-Santos, D.V., Rao, P.K., Davies, J.B., Sohn, E.H., Rao, N.A., 2010. Clinical features of tuberculous serpiginouslike choroiditis in contrast to classic serpiginous choroiditis. Archives Ophthalmol. 128 (7), 853–858.
Vogt, A., 1906. Fruhzeiiges ergrauen der Zilien und Bemerkungen uber den sogenannten plotzlichen Eintritt diaser Veranderung. Klin. Monatsbl Augenheilkd 44, 228–242.
Wakefield, D., Lloyd, A., 1992. The role of cytokines in the pathogenesis of inflammatory eye disease. Cytokine 4, 1–5.
Walton, R.C., Ashmore, E.D., 2003. Retinal vasculitis. Curr. Opin. Ophthamol 14, 413–419.
Watzke, R.C., 1984. Punctate inner choroidopathy. Am. J. Ophthalmol. 98 (5), 572–584.
Watzke, R.C., Packer, A.J., Folk, J.C., Benson, W.E., Burgess, D., Ober, R.R., 1984. Punctate inner choroidopathy. Nov Am. J. Ophthalmol. 98 (5), 572–584.
Weinhaus, R.S., Burke, J.M., Delori, F.C., Snodderly, D.M., 1995. Comparison of fluorescein angiography with microvascular anatomy of macaque retinas. Jul Exp. Eye Res. 61 (1), 1–16.
White, B.R., Pierce, M.C., Nassif, N., 2003. In vivo dynamic human retinal blood flow imaging using ultra-high-speed spectral domain optical coherence tomography. Opt. Express 11, 3490–3497.
Wiechens, B., Nölle, B., 1999. Iris angiographic changes in multifocal chorioretinitis with panuveitis. Nov Graefes Arch. Clin. Exp. Ophthalmol. 237 (11), 902–907.
Yamamoto, S., Hayashi, M., Tsuruoka, M., Yamamoto, T., Tsukahara, I., Takeuchi, S., 2003. S-cone electroretinograms in multiple evanescent white dot syndrome. Mar Doc. Ophthalmol. 106 (2), 117–120.
Yannuzzi, L.A., Rohrer, K.T., Tindel, L.J., Sobel, R.S., Costanza, M.A., Shields, W., Zang, E., 1986 May. Fluorescein angiography complication survey. Ophthalmology 93 (5), 611–617.
Yanoff, M., Fine, B.S., Brucker, A.J., Eagle Jr., R.C., 1984. Pathology of cystoid macular edema. Surv. Ophthalmol. 28 (Suppl. l), 501–511.
Zahid, S., Chen, K.C., Jung, J.J., Balaratnasingam, C., Ghadiali, Q., Soreson, J., Rofagha, S., Freund, K.B., Yannuzzi, L.A., 2016. Optical coherence tomography angiography of chorioretinal lesions due to idiopathic multifocal choroiditis. Retina [Epub ahead of print].